Aus der Urologischen Klinik und Poliklinik der

Ludwig-Maximilians-Universität München

Direktor: Prof. Dr. med. Christian G. Stief

Identification of new prognostic markers in renal cell carcinoma

Dissertation

zum Erwerb des Doktorgrades der Medizin

an der Medizinischen Fakultät der

Ludwig-Maximilians-Universität zu München

vorgelegt von

Dong Chen

aus

Fujian, China

2014

Mit Genehmigung der Medizinischen Fakultät

der Universität München

Berichterstatter:	Prof. Dr. med. Christian. G. Stief
Mitberichterstatter:	Prof. Dr. med. Dirk Zaak
	Priv. Doz. Dr. med. Florian May
Mitbetreuung durch den Promovierten Mitarbeiter:	Priv. Doz. Dr. med. Alexander Buchner
Dekan:	Prof. Dr. med. Dr. h.c. M. Reiser, FACR, FRCR
Tag der mündlichen Prüfung:	27.03.2014

Publications that contain results from this thesis:

Expression and prognostic significance of a comprehensive epithelial-mesenchymal transition gene set in renal cell carcinoma.

Chen D, Gassenmaier M, Maruschke M, Riesenberg R, Pohla H, Stief CG, Zimmermann W, Buchner A.

J. Urol. 2014; 191(2): 479-86

CXC chemokine receptor 4 is essential for maintenance of renal cell carcinoma-initiating cells and predicts metastasis.

Gassenmaier M, Chen D, Buchner A, Henkel L, Schiemann M, Mack B, Schendel DJ, Zimmermann W, Pohla H.

Stem Cells 2013; 31(8):1467-76

Contents

1. Introduction

1.1 Objective of the study

Globally, there are 270,000 new cases of kidney cancer diagnosed yearly and approximately 90% of all kidney cancers are clear cell renal cell carcinoma (RCC). About 20-30% of all patients have metastatic disease at time of diagnosis, and another 20% of patients undergoing nephrectomy will develop metastases during follow-up (Ljungberg, Campbell et al. 2011). Therefore, it is of vital importance to find effective prognostic markers and new therapeutic targets to enable risk stratification and individualized therapeutic strategy in RCC patients.

The objective of this study was the identification of novel independent prognostic markers and potential therapeutic targets in clear cell RCC, based on a biobank with patients' tissue samples, histopathological information and the corresponding follow-up data. Various approaches were used for selection of promising candidate genes: Epithelial-mesenchymal transition (EMT) is an established theory for interpretation of tumor invasion and tumor metastasis in solid tumors. Since there is almost no data available about the role of EMT in RCC and about its potential impact on the outcome, EMT-related genes were in the focus of this study. Additionally, genes related to cancer stem cells, organ size controlling Hippo pathway, and CXCR4 signaling pathway were analyzed in this study. Details of EMT and the other investigated pathways are provided in the following sections.

1.2 Epithelial-mesenchymal transition

Carcinoma cells undergo a characteristic change from an epithelial to a mesenchymal cell-like phenotype called epithelial-mesenchymal transition (EMT) during cancer progression (Figure 1) (Polyak and Weinberg 2009, Thiery, Acloque et al. 2009, Tiwari, Gheldof et al. 2012). This kind of cell

phenotype change can facilitate tumor cell migration and invasion at an early stage of tumor development and form distant metastasis (Rhim, Mirek et al. 2012). Increasing evidence supports the notion that the dynamic process of EMT gives rise to tumor cell dissemination and, together with mesenchymal-epithelial transition (MET), the reversal of EMT, finally leads to outgrowth of metastases (Brabletz 2012, Tsai, Donaher et al. 2012). More recently, it has been shown that the mesenchymal properties gained during EMT are shared by cancer stem cells (Mani, Guo et al. 2008). This is clinically highly relevant since cancer stem cells are thought to selectively survive chemotherapy due to their insensitivity to drugs which can lead to disease relapse (Singh and Settleman 2010). In addition, EMT genes attract interest for their clinical significance as prognosis predictors or potential therapeutic targets (Iwatsuki, Mimori et al. 2010, Singh and Settleman 2010). Based on the EMT theory, mesenchymal cell markers such as vimentin and fibronectin 1 should be up-regulated during the process of tumorigenesis, while the epithelial cell markers, such as E-cadherin, will lose the expression density. This process was recognized as a loss of cell polarity, stability and gain of migration and invasion ability in cancer cells. EMT is mostly under transcriptional control. Important players of EMT are master transcription factors like ZEB and SNAIL family members which can induce EMT upon overexpression (De Craene and Berx 2013). Loss of cell adhesion molecule E-cadherin expression mediated by transcriptional repression of CDH1 (encoding E-cadherin) through ZEB and SNAIL transcription factors and induction of extracellular matrix-degrading metalloproteinase (MMPs), such as MMP2 and MMP9, are hallmarks of EMT that facilitate the invasive phenotype (De Craene and Berx 2013). The EMT process can be induced by cytokines and growth factors such as transforming growth factor ß (TGF-ß) which are produced by the tumor stroma or possibly by the tumor cells (Heldin, Vanlandewijck et al. 2012).

It is widely accepted that EMT plays an important role in a number of solid tumors (Thiery, Acloque et al. 2009, Iwatsuki, Mimori et al. 2010).

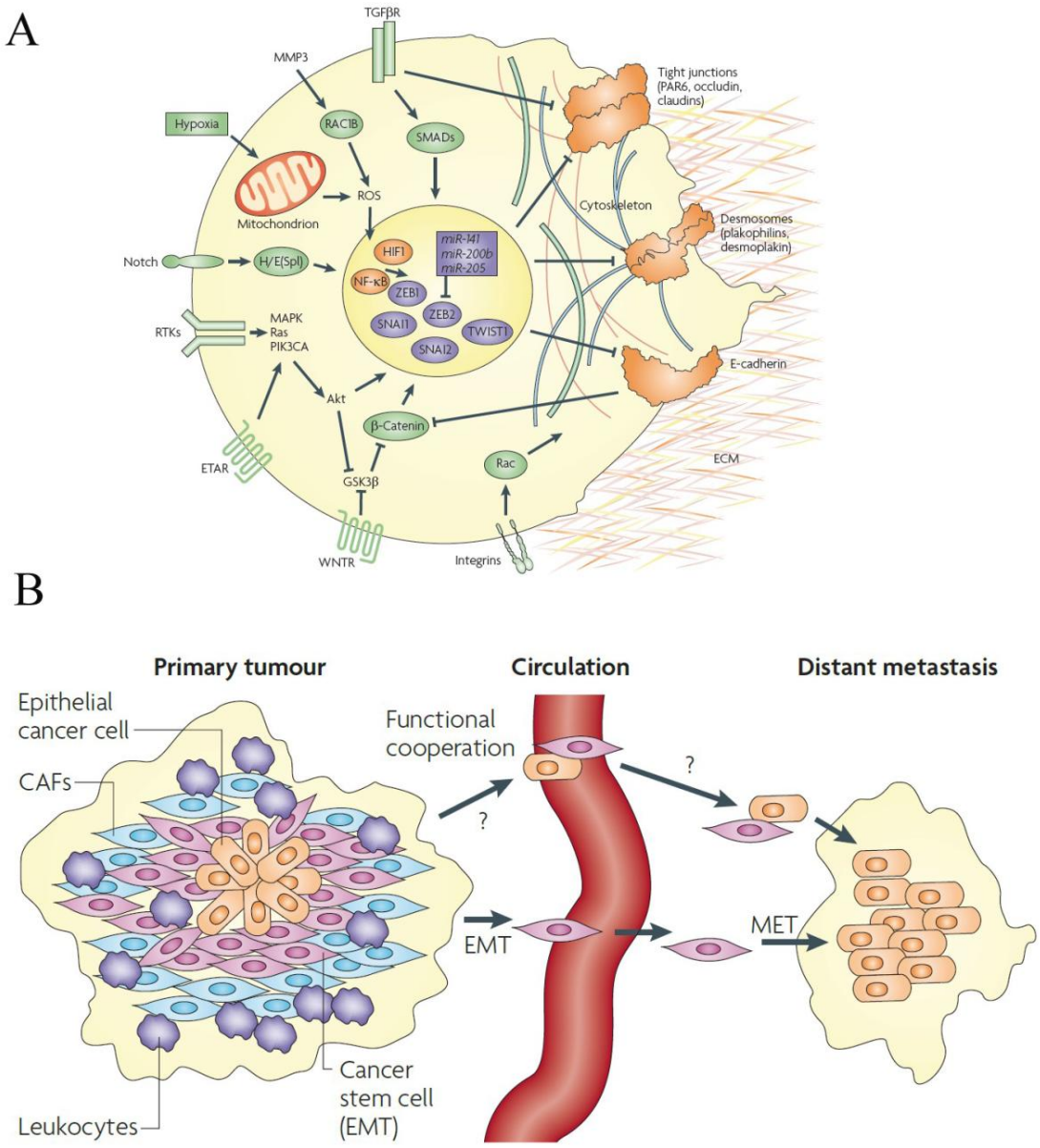

Figure 1: Overview of Epithelial-mesenchymal transition: (A) simplified overview of signaling networks regulating epithelial–mesenchymal transition (EMT). (B) Transitions between epithelial and mesenchymal states during carcinoma progression. In the primary tumor, EMT and mesenchymal-epithelial-transition (MET) contribute to intratumoral heterogeneity. Interactions with stromal cells, including leukocytes and cancer-associated fibroblasts (CAFs), may induce EMT. Macroscopic distant metastases are frequently composed of more differentiated epithelial cancer cells. This may be explained by MET, a reversal of EMT, after macrometastases grow. Functional cooperation of cancer stem cells and epithelial cancer cells are not well established. (Polyak and Weinberg 2009)

1.3 Molecular links between cancer stem cells and epithelial-mesenchymal transition during metastasis

From a biological point of view metastasis in various solid tumors is comprised by several distinct steps named "invasion-metastasis cascade". This cascade includes gain of traits like invasiveness leading to immigration into surrounding tissues and lymphatic and blood vessels (intravasation), exit from vasculature (extravasation), and finally enhanced survival and proliferation in the foreign environment to form metastases (colonization) (Aktas, Tewes et al. 2009, Geiger and Peeper 2009).

In the early stage of metastasis, primary tumor cells need to invade and disseminate from the primary tumor which needs coordination of transcription factors such as TWIST, SNAIL, SLUG, and ZEB1 to repress expression of epithelial adhesion molecules such as E-cadherin. At the same time, mesenchymal components such as N-cadherin, vimentin and fibronectin are up-regulated. After intravasation and extravasation, cancer cells need to adapt to the colony environment and grow as metastasis. In this stage, stem cell properties of self-renewal, tumor-initiating and high proliferation capacity are taking place.

Taken together, cells which successfully escape from the primary tumor and colonize distant organs are supposed to undergo an EMT process in an early stage to gain mesenchymal traits and also gain cancer stem cell properties to finally leading to clinical progression.

Many details of the biological process of metastasis in RCC are still unclear. Identification of biomarkers which can be used as independent prognostic predictors or therapeutic targets is crucial for RCC patients. For basic research, it is also important to investigate promising genes involved in RCC metastasis and to clarify the mechanism of tumor metastasis. Since no clear boundary between EMT and stem cell

properties can be defined and many genes were reported to be involved in both, genes which are related to these two processes were selected as promising targets in this study.

Given the essential role of EMT for tumor progression in other carcinomas and the limited information available for RCC, we decided to comprehensively analyze EMT-associated gene expression in RCC. Because EMT is a transcriptionally regulated differentiation process, we used transcriptome analysis and RT-PCR to quantify EMT-related gene expression. We assembled a list of 46 genes which were reported in literature to be up-regulated during EMT in different epithelial cancers.

1.4 Trophoblast glycoprotein (TPBG), CXCR4 and EMT

Functional interaction of TPBG (previously known as 5T4) and the tumor stem cell marker CXCR4 has been reported previously. However, the mechanisms behind are still not completely resolved. Since TPBG shows high expression in malignant tissues and promising results as a therapeutic target (Shaw, Connolly et al. 2007, Elkord, Shablak et al. 2009, Tykodi, Satoh et al. 2012), it was selected as a candidate in this study too. CXCR4 has been recognized as a tumor stem cell marker in various epithelial tumors, and interaction between CXCR4 and EMT has been reported (Onoue, Uchida et al. 2006, Li, Ma et al. 2012, Gassenmaier, Chen et al. 2013). Therefore, it was also selected for analysis in this study.

1.5 Another investigation approach: identification of progression related genes by microarray data analysis

Additionally to the focus on EMT-related genes including TPBG and CXCR4, a second strategy was used in this study to identify new prognostic markers in RCC: microarray expression data from RCC patients including normal kidney tissues from tumor-bearing kidney, primary tumors and metastases were analyzed to screen for promising

prognostic markers using a novel filtering approach, based on genes that are subsequently up-regulated in primary tumors and metastases.

In this approach, the hypothesis is as follows: in the tumor progression sequence “normal kidney tissue – primary tumor – metastases”, genes that show increasing expression in a progression-dependent way could be especially important for RCC biology and therefore interesting for further research.

In principle, these genes can encode either harmful or protective factors during tumor progression. Regardless of the biological role of these molecules, they might also be interesting for this study by coding for prognostic factors in RCC patients.

2. Materials and Methods

2.1 Materials

2.1.1 Cell lines

HEK-293T cells (human embryonic kidney) were used for as control in transfection experiments. RCC cell lines RCC53 (Djafarzadeh, Noessner et al. 2006) and SK-RC-17 (Ebert, Bander et al. 1990) were kindly provided by PD Dr. Heike Pohla, Tumor Immunology Laboratory, LIFE Center, LMU, München.

2.1.2 Patient tissues

Tissue samples from primary tumors and metastases were collected from clear cell renal cell carcinoma (RCC) patients undergoing surgical resection of RCC at two different centers. A total of 42 samples including 14 normal tissues from tumor-bearing kidneys, 28 primary tumors (14 grade G1 and G3 tumors each) were used for microarray analysis (Department of Urology, University of Rostock). The characteristics of this microarray patient cohort are summarized in Table 1. Another 112 tissue samples from 82 patients with clear cell RCC were used for real-time PCR analyses, including 19 normal tissues from tumor-bearing kidneys, 55 primary tumors and 38 metastases from various locations which were used for survival analysis. 32 metastases (those with the best RNA quality) were also used for microarray analysis with the normal-primary-metastases comparison approach. From each patient and site, one tissue sample was analyzed. The patients underwent tumor nephrectomy, partial nephrectomy or resection of metastases between 1992 and 2011 at the Department of Urology, University of Munich. The characteristics of these patients are summarized in Table 2. The median follow-up time was 54 months. Staging was performed according to the Ficarra TNM

classification (Sobin L 2009). Normal tissue samples were taken from tumor-bearing kidneys and approved by a pathologist to be histologically normal. All patients gave informed consent, and the research was approved by the local ethics committees.

Table 1: Patient characteristics: Cohort of Rostock (Maruschke, Hakenberg et al. 2013)

	Primary G1 n (%)	Primary G3 n (%)
Total no. patients	14	14
Age (years)		
Median (range)	65 (53–77)	59 (48–79)
Sex (%)		
Male	8 (57)	9 (64)
Female	6 (43)	5 (36)
Pathological stage (%)		
pT1–2	13 (93)	3 (21)
pT3a	1 (7)	3 (21)
pT3b	0 (0)	8 (58)
pT4	0 (0)	0 (0)
Pathological nodal status (%)		
Negative	14 (100)	10 (71)
Positive	0 (0)	3 (21)
Unknown (pNX)	0 (0)	1 (8)
Distant metastases (%)		
M0	14 (100)	3 (21)
M1	0 (0)	11 (79)
Tumor grade (%)		
G1	14 (100)	0 (0)
G2	0 (0)	0 (0)
G3	0 (0)	14 (100)
Normal renal tissue available (%)	8 (57)	6 (43)

Table 2: Patient characteristics of RT-PCR: Cohort of Munich

	Classification	Primary tumors: n (%)	Metastases: n (%)
T			
	T1-T2	29 (52.7)	12 (31.6)
	T3-T4	26 (47.3)	26 (68.4)
N			
	N0	41 (74.5)	22 (57.9)
	N+	10 (18.2)	11 (28.9)
	NX	4 (7.3)	5 (13.2)
M			
	M0	26 (47.3)	16(42.1)
	M1	29 (52.7)	22 (57.9)
G			
	G1-G2	45 (81.8)	22 (57.9)
	G3	10 (18.2)	16 (42.1)
Age			
	<60	22 (40.0)	23 (60.5)
	≥60	33 (60.0)	15 (39.5)
Gender			
	Male	32 (58.2)	23 (60.5)
	Female	23 (41.8)	15 (39.5)
Metastatic Site (%)	Adrenal gland		12 (31.6)
	Lymph node		12 (31.6)
	Lung		7 (18.4)
	Liver		4 (10.5)
	Cava		2 (5.3)
	Brain		1 (2.6)

2.1.3 Primers

All primers were designed using the online tool primer-blast (http://www.ncbi.nlm.nih.gov/tools/primer-blast/) (Ye, Coulouris et al. 2012). Primers were supplied by Eurofins (Ebersberg, Germany); sequences and product sizes are listed in Table 3. Quality control was performed for all primers. Primers were only used for RT-PCR when the melting curve of the amplified products had only one peak, and when only one clear band of product with the expected size was detected by agarose gel electrophoresis.

Table 3: Oligonucleotides used for RT-PCR

Primer ID	**Sequence (5'→3'):**	**Product size (bp)**
AMPD3_f	TTGCAGAGACAGGGACTGG	116
AMPD3_r	AAAAGGAAGCCAAGGAGAGG	
ATAD2_f	TCCGGTGGTAGGTTTCAACT	130
ATAD2_r	TTCCTCAGTCTGGAGCACATC	
AURKA_f	GCTGGAGAGCTTAAAATTGCAG	141
AURKA_r	TTTTGTAGGTCTCTTGGTATGTG	
BUB1B_f	CCAGGCTTTCTGGTGCTTAG	148
BUB1B_r	CTCGTGGCAATACAGCTTCA	
CDH1_f	GAATGACAACAAGCCCGAAT	88
CDH1_r	GACCTCCATCACAGAGGTTCC	
CDH2_f	GGTGGAGGAGAAGAAGACCAG	71
CDH2_r	GCATCAGGCTCCACAGT	
CDT2/DTL_f	CCATATCCCTGAGGACTGTGT	282
CDT2/DTL_r	TTCCCAAAGCCCAACAGTCA	
CENPF_f	TTGTAAAGAAAGGGTTTGC	172
CENPF_r	CCAGCTGTTGGTTTGGAGG	
CXCL12_f	ACTGGGTTTGTGATTGCCTCTGAA	150
CXCL12_r	GGAACCTGAACCCCTGCTGTG	
CXCR4_f	TGGGTGGTTGTGTTCCAGTTT	80
CXCR4_r	ATGCAATAGCAGGACAGGATGA	
CXCR7_f	TACCCCGAGCACAGCATCAA	82
CXCR7_r	TGGAGAAGGGAACGGCAAAG	
FN1_f	AAACCAATTCTTGGAGCAGG	142
FN1_r	CCATAAAGGGCAACCAAGAG	
GAPDH_f	CAACTACATGGTTTACATGTTC	180
GAPDH_r	GCCAGTGGACTCCACGAC	
HELLS_f	CCCTCCTTTCTTCTAGTAATGCAGTT	81
HELLS_r	CCCAATCTCTCCCCATGAAAA	
MMP2_f	TTGATGGCATCGCTCAGATC	82
MMP2_r	TTGTCACGTGGCGTCACAGT	
MMP9_f	GCAAGCTGGACTCGGTCTTT	64
MMP9_r	TGGCGCCCAGAGAAGAAG	
NDC80_f	AGGACCTGGAAGCTGAACAA	75
NDC80_r	TTTCAATCGCTTCTTTGCCT	
S100A4_f	GGCTTGCACACGCTGTTGCT	71
S100A4_r	GCCTTCTCCAGAGGGCACGC	
SFN_f	GAGGAAACATGGTCACACCC	134
SFN_r	TGAGAACTGGACAGTGGCAG	

SLUG_f	TGTTGCAGTGAGGGCAAGAA	72
SLUG_r	GACCCTGGTTGCTTCAAGGA	
SYBU/GOLSYN_f	TTCTTCACGCAATCGAGGTCC	207
SYBU/GOLSYN_r	GGGCTACAGTCGCTTCCTTT	
TET3_f	TCCAGCAACTCCTAGAACTGAG	169
TET3_r	AGGCCGCTTGAATACTGACTG	
TOP2A_f	CATTGAAGACGCTTCGTTATGG	104
TOP2A_r	CCAGTTGTGATGGATAAAATTAATCAG	
Twist_f	TGTCCGCGTCCCACTAGC	93
Twist_r	TGTCCATTTTCTCCTTCTCTGGA	
VIM_f	AAAGTGTGGCTGCCAAGAAC	74
VIM_r	AGCCTCAGAGAGGTCAGCAA	
ZEB1_f	GCCAATAAGCAAACGATTCTG	101
ZEB1_r	TTTGGCTGGATCACTTTCAAG	
ZEB2_f	GCGGCATATGGTGACACACAA	81
ZEB2_r	CATTTGAACTTGCGATTACCTGC	

2.1.4 Antibodies, plasmids, chemicals, bacteria and antibiotics

All reagents and bacteria used in the study are listed in Table 4.

Table 4: Materials used in this study

	Catalog No.	**Company**
Antibodies:		
Anti-CXCR4 monoclonal rabbit antibody, clone UMB2	ab124824	Abcam plc.
Anti-human CXCR4 Antibody monoclonal mouse antibody (IgG2B), Clone 44716	MAB172	R&D Systems
Anti-CXCR4 polyclonal rabbit antibody	Ab2074	Abcam plc.
Anti-human CXCR4 polyclonal rabbit antibody	19490002	Novus Biologicals.
Anti-MMP2 monoclonal mouse antibody (IgG1), clone 4D3	ab2462	Abcam plc.
Anti-human 5T4 monoclonal mouse antibody (IgG1), Clone 524731	MAB4975	R&D Systems
Anti-mouse CD184/CXCR4 PE monoclonal rat antibody (IgG2b)	12-9991-81	eBioscience
Anti-human 5T4-APC monoclonal mouse antibody (IgG1), clone 524744	FAB49751A	R&D Systems
Anti-topoisomerase II alpha monoclonal rabbit antibody (IgG), clone EP1102Y	ab52934	Abcam plc.

Anti-TET3 polyclonal rabbit antibody	PA5-34431	Thermo Fisher Scientific Inc.
Anti-human Ki-67 monoclonal mouse antibody, clone MIB-1	M7240	Dako
Anti-Lsh mouse monoclonal antibody (IgG2a), clone H-4	sc-46665	Santa Cruz Biotechnology
Anti-ZEB1 monoclonal mouse antibody (IgG2a), clone 4C4	H00006935-M01	Abnova Corporation.
Anti-ß-actin monoclonal mouse antibody (IgG2a), clone AC-74	A5316	Sigma-Aldrich Co.
Anti-mouse IgG (H and L Chain) polyclonal goat antibody, peroxidase-conjugated	401215	Calbiochem
Anti-mouse IgG polyclonal goat antibody (H and L chain), Alexa Fluor® 633-conjugated	A21050	Life Technologies
Other compounds:		
AMD3100 octahydrochloride	3299	TOCRIS bioscience
Recombinant CXCL12/SDF-1a, CF	350-NS/CF	R&D Systems
Transfection materials:		
pCMV6-XL5-human TPBG contains Homo sapiens trophoblast glycoprotein , transcript variant 1 as transfection-ready DNA	SC115948	OriGene Technologies
pCMV-SPORT6-human CXCR4	IRAVp968H08146D	Source BioScience
Fusin siRNA, 10 mM	sc-35421	Santa Cruz
Control siRNA-A; 10 mM	sc-37007	Santa Cruz
siRNA Transfection Reagent, 0.3 ml	sc-29528	Santa Cruz
siRNA Transfection Medium, 20 ml	sc-36868	Santa Cruz
siRNA Dilution Buffer, 1.5 ml	sc-29527	Santa Cruz
FuGENE® 6 Transfection Reagent	11815091001	Roche
X-tremeGENE HP DNA Transfection Reagent	06 366 244 001	Roche
QIAquick PCR Purification Kit	28104	QIAGEN
QIAprep Spin Miniprep Kit	27104	QIAGEN
NucleoBond® Xtra Maxi Plus	740416.10	MACHEREY-NAGEL GmbH
Cell biology experiments materials:		
RPMI 1640	21875-034	Gibco
PBS, sterile	10010-015(056)	Gibco
Accutase	L11-007	PAA
Inserts for 24-well plates	353097	BD Biosciences
BD Matrigel™ Basement Membrane	354262	BD Biosciences

Matrix High Concentration, Phenol Red Free, 10 ml vial		
L-Glutamine 200mM(100x), 100 ml	25030-024	Life Technologies
MEM Non-Essential Amino Acids(100x), 100 ml	11140-035	Life Technologies
Sodium Pyruvate MEM 100 mM, 100 ml	11360-039	Life Technologies
Acetone ACS grade, 2.5 liter	1.00014.2500	Merck
Methanol ACS grade, 2.5 liter	106009.2500	Merck
CellTiter-Blue® Cell Viability Assay	G8081	Promega Corporation.
µ-Dish 35 mm, high Culture-Insert	81176	ibidi
7-Amino-actinomycin D (7-AAD) staining solution	559925	BD Biosciences
HEPES, 1M, 20 ml	15630-049	Gibco
EDTA, 0.5M, 100 ml	AM9260G	Ambion
Ultra-Low Attachment flask: 25/75 cm²	3471	Corning
DMEM/F12	1221806	Gibco
Insulin-transferrin-selenium-x (ITS-x), 100x	51500-056	Gibco
B 27	17504-044	Invitrogen
Basic fibroblast growth factor (bFGF)	F0291	Sigma
Epithelial growth factor (EGF)	PHG0311	Life Technologies
Immunochemistry materials:		
Hematoxylin Solution	HHS16-500ML	Sigma
ImmPRESS Universal Antibody (anti-mouse Ig/anti-rabbit Ig, peroxidase) Polymer Detection Kit	MP-7500	Vector Laboratories
ImmPACT AEC Peroxidase Substrate	SK-4205	Vector Laboratories
BLOXALL Endogenous Peroxidase and Alkaline Phosphatase Blocking Solution	SP-6000	Vector Laboratories
Western blotting (WB) materials:		
Coomassie (Bradford) protein Assay Kit	23200	Thermo Fisher Scientific Inc.
SuperSignal® West Pico Chemiluminescent Substrate	34079	Thermo Fisher Scientific Inc.
NuPAGE® Bis-Tris Mini Gels	IM-8042	Life Technologies Corporation
NuPAGE® Transfer Buffer(20x)	NP0006	Life Technologies
NuPAGE® RunningBuffer(20x)	NP0001	Life Technologies

Precision Plus Protein Dual Color Standards, 500 µl	161-0374	Bio-Rad
GE Healthcare AmershamHyperfilm ECL	28906837	Amersham
DL-Dithiothreitol (DTT), 1 g	D9163	Sigma-Aldrich, Inc.
Real-time PCR materials:		
RNeasy Mini Kit	74104	QIAGEN
LightCycler® FastStart DNA Master plus SYBR Green I Kit	03515885001	Roche
Reverse Transcription System	A3500	Promega Corporation.
QIAshredder Kit	79654	QIAGEN
RNA 6000 Pico Assay	50671513	Agilent Technologies
Gene Ruler 100bp DNA ladder	SM0241	Fermentas
Gene Ruler 1kb DNA ladder	SM0311	Fermentas
6x DNA Loading Dye, 1 ml	R0611	Fermentas
99% Ethanol	100990	Merck
ß-ME	M3148	Sigma
UltraPure™ Agorose, 500 g	16500500	Life Technologies
UltraPure™ 10 x TAE buffer	15558042	Life Technologies
Ethidium Bromide Solution, 10 mg/ml	161-0433	Bio-rad

2.1.5 Buffers and solutions

The following buffers and solutions were made for different experiments:

Lysogeny broth (LB) media (a total of 1 liter) contains: 10 g Bacto-Tryptone, 5 g Bacto-Yeast extracts and 5 g NaCl. The pH value is 7.5. Solution was sterilized by autoclaving and stored at room temperature.

LB media (a total of 1 liter) contains: 15 g Bacto-Agar, autoclaved and stored at 4°C.

Ampicillin: 100 mg/ml (stock solution, -20°C), 1:1000 diluted in agar to a concentration of 100 µg/ml.

SOC Media contains: 800 ml deionized H_2O, 20 g Bacto-Tryptone, 5 g Bacto-Yeast Extract and 0.5 g NaCl.

10x PBS / for Western blotting contains (a total of 1 liter): 80 g/l NaCl, 2 g/l KCL, 11.5 g/l Na_2HPO_4 or 14.8 g/l Na_2HPO_4-$(H_2O)_2$, 2 g/l KH_2PO_4 and adjusted to 1 liter with distilled water.

Protein lysis buffer stock solution contains: 50 mM Tris-HCl (pH 8.0, 1 ml Tris-HCL plus 19 ml nuclease free water), 150 mM NaCl (8.77 g/l, 175.4 mg for 20 ml), 1% Triton X-100 (200 µl for 20 ml) and "Complete Mini-Protease Inhibitor Cocktail"(1 tablet for 1.5 ml lysis buffer).

Running buffer for WB contains: 10 ml 20x running buffer plus 190 ml dH_2O.

Transfer buffer for WB contains: 10 ml 20x buffer, 20 ml Methanol and 170 ml H_2O.

Blocking milk buffer: 25 g (5%) skim milk powder + 50 mL 10x PBS + 500 µl Tween 20 adjusted to 500 ml with dH_2O.

1x TBS contains: 50 mM Tris pH 8.0, 138 mM NaCl, 2.7 mM KCl.

1x TBS-T (a total of a liter) contains: 1 liter 1x TBS, 500 µl Tween 20.

Gel for DNA-fragment analysis: 2% agarose dissolved in 100 ml TBS buffer, cool down and add 1 µl ethidium bromide (EtBr; 10 mg/ml); pour in tray of electrophoresis apparatus for solidification.

Cell culture standard media: RMPI 1640 media 500 ml, 50 ml FBS, 5 ml MEM, 5 ml sodium pyruvate and 5 ml L-glutamine.

Sphere formation assay media: DMEM/F12 96.84%, ITS-X 1% (v/v), B27 2% (v/v), bFGF 0.08%, EGF 0.08%.

FACS buffer (for 40 ml): 38.28 ml PBS, 1 ml of 1 M HEPES, 320 µl of 0.5 M EDTA and 400 µl FBS.

2.1.6 Apparatus and software

Apparatus and software used in the study are listed below: BZ-8000 microscope (Keyence Corporation, Osaka, Japan); Light Cycler 96 (Roche, Penzberg, Germany); High-speed Centrifuge (Eppendorf, Hamburg, Germany), Bioanalyzer 2100 (Agilent, Böblingen, Germany); NanoDrop 2000 (Thermo Fisher Scientific); Peltier Thermal Cycler DNA Engine PTC-200 (Bio-Rad, Munich, Germany); Fluor-S™ MultiImager (Bio-Rad, Munich, Germany); Horizontal Gel Electrophoresis System (Gibco / Life Technologies, Darmstadt, Germany); Thermomixer comfort (Eppendorf, Hamburg, Germany); FACS Calibur™ (BD Bioscience, Heidelberg, Germany); Cell Quest Pro software (BD Bioscience, Heidelberg, Germany); FlowJo (Tree Star Inc., Ashland, OR, USA).

2.2 Cell culture

The human renal cell carcinoma cell lines RCC53 and SK-RC-17 and the human embryonal kidney cell line HEK-293T were obtained from the Tumor Immunology Laboratory, LIFE Center of Klinikum Großhadern. All cells were recovered from liquid nitrogen and maintained in RPMI 1640 media (Invitrogen, Life Technologies GmbH, Darmstadt, Germany) supplemented with 10% FBS (Biochrom AG, Cambridge, UK), 1% MEM non-essential amino acids, 1 mM sodium pyruvate, and 2 mM L-glutamine (all from Invitrogen, Life Technologies GmbH, Darmstadt, Germany). Cells were cultured at 37°C in a humidified atmosphere containing 5% CO_2 and passaged by Accutase (PAA Laboratories, Freiburg, Germany) detachment. Before detachment, cells were washed with water-bath (37°C) pre-warmed PBS (Invitrogen, Life Technologies GmbH, Darmstadt, Germany) to get rid of the culturing media. After incubation for 5 min in 1 ml Accutase at 37°C, 10 ml (10-fold excess) of pre-warmed (37°C) complete culturing media was added to block the digestion process, and cells were

collected by centrifugation (1,200 rpm, 5 min). Cell pellets were then re-suspended using complete media and transferred to new flasks. For freezing and thawing of cells, detached cells after Accutase digestion were centrifuged and re-suspended in 1ml freezing media (FBS supplemented with 10% DMSO) and transferred into a cryotube, then stored at -80°C for short term storage (1 month) or nitrogen tank for long term storage.

2.3 Plasmid transformation, preparation, validation and transfection

2.3.1 Plasmid DNA transformation

Transformation of competent cells with plasmid DNA

- Remove 20 or 25 µl bacteria aliquot from -80°C and let thaw on ice (it is important to keep competent cells cool). Give first of each ligation mixture 2 (2.5) µl to 20 (25) µl bacterial suspension, mix briefly in 2 ml Eppendorf tube, then incubate for 30 min on ice.
- When plasmid was obtained on blotting paper, then dissolve the DNA in 30 µl of water (transfer paper into Eppendorf tube), leave for 10 min, then centrifuge for 1 min, remove paper. For transformation, use similar quantity as above.
- For control (positive control), add 50 ng of vector in 1 µl to 25 µl bacteria aliquot.
- Incubate for heat shock 45 s at 42°C, then immediately transfer to ice for 2 min (minimum time) followed by adding 125 µl of pre-warmed (42°C) SOC media (Invitrogen). Then shake in a shaker at 37°C for 1 h at 650 rpm.
- Spread on LB agar plates containing the appropriate antibiotic (e.g., 100 µg/ml ampicillin). Tip: Spread by evenly spreading cells over the

plate using a "hockey puck" spreader. Be sure that you have dipped your spreader in ethanol and flamed it before spreading.

- Place in the 37°C incubator with the lid side down. Incubate overnight then transfer to refrigerator (4°C) sometime the next day.

2.3.2 Maxi preparation

- Pick single clone and add it in 100 ml of LB media.
- Incubate at 37°C, shaking (200 rpm) over night
- Perform plasmid DNA purification using NucleoBondXtra, Maxi Plus according to the manufacturer's instructions.

2.3.3 Restriction endonuclease digestion and DNA purification

For enzyme digestion, mix and spin down:

35 µl nuclease free water
5 µl 10x Fast Digest Buffer
5 µl plasmid DNA
5 µl *Not*I Fast Digest enzyme

→ 37°C for 1 h, followed by 80°C, 10 min to inactivate the enzyme

QIAquick PCR Purification Kit:

- Add 5 volumes PB Binding Buffer to 1 volume of PCR sample: add 250 µl PB Binding Buffer to 50 µl PCR sample
- Transfer DNA binding column to 2 ml collection tube, fill with mixed sample, and centrifuge for 1 min at 13,000 rpm.
- Discard flow-through and put column back into the same tube.
- Add 750 µl PE buffer to the column for washing and centrifuge for another 1 min.
- Discard flow-through and put column back into the same tube.

- Centrifuge the column again for 1 min to completely remove the residual alcohol containing PE buffer (might interfere with later use).
- Transfer QIAquick column into a new 1.5 ml microcentrifuge tube (Eppendorf tube).
- For the extraction of DNA, pipette 30 µl of EB buffer onto the center of the membrane, let stand for 1 min, then centrifuge for 1 min.
- Discard column, store purified DNA at -20°C and check the length using gel of DNA fragment using gel electrophoresis.

2.3.4 Transfection

One day before transfection, cells were seeded in 6-well plates. Cells were cultured to 60-80% confluence. Plasmid DNA transfection solution was prepared as follows: 97 µl RPMI, 3 µl Fugene transfection reagent, 2 µl plasmid DNA per well of 6-well plate. Allow to stand for 30 min, and then fill up with 6 ml RPMI. Aspirate the old medium and fill each well with 1 ml of transfection solution. Forty-eight h after transfection, cells can be analysed for protein expression by flow cytometry (see 2.4) or Wetern blot (see 2.7).

2.4 Flow cytometry (FC)

Flow cytometry was used to measure the cell membrane expression of TPBG and CXCR4.

2.4.1 Cell preparation and flow cytometry

- Harvest cells from 70-90% confluent cells in T75 flask
- Spin cells down (1,200 rpm, 5 min)
- Count cells
- Re-suspend $5x10^5$ cells in 100 µl FACS buffer

- Stain cells with 10 µl anti-CXCR4 (PE) or 10 µl anti-TPBG (APC) antibody for 30 min at room temperature in the dark (briefly vortex in between)
- Wash cells with 600 µl FACS buffer
- Centrifuge cells (1,500 rpm, 5 min)
- Re-suspend cells in 100 µl FACS buffer
- Add 5 µl 7-AAD (concentration as supplied) for live/dead discrimination
- Store the cells for 10 min in the fridge in the dark until analysed

2.4.2 Setup, data acquisition and analysis

- Switch on FACS Calibur first and then computer
- Start software: FACS Pro
- Acquire-connect to cytometer
- Acquire/parameter Description: P1 for FSC, P2 for SSC, P4 for PE staining, P5 for 7-ADD staining, and P7 for APC staining.
- Set directory and file count
- Adjust cytometer/instrument setting
- For data acquisition, count more than 20,000 events
- Data analysis is done using FlowJo software (Tree Star. Inc., Ashland, USA)

2.5 Quantitative PCR

2.5.1 RNA isolation and concentration measurement

- Prepare: Buffer RLT containing ß-ME (add 10 µl ß-ME to 1 ml RLT); Buffer RPE(add 96-100% ethanol as required by the manufacturer); 70% ethanol
- Tissue amount should be less than 30 mg.
- Add 600 µl RLT buffer to tissue(storage up to 1 month at room temperature)

- Transfer to QIAshredder, centrifuge for 2 min, maximum speed, transfer supernatant to column
- Add 600 µl 70% ethanol to supernatant and mix by pipetting (do not centrifuge)
- Add 700 µl mixed sample to column inserted in a Eppendorf tube (2 ml), centrifuge for 15 s, maximum speed, discard the flow-through
- Add 700 µl RW1 buffer to column, centrifuge for 15 s, maximum speed, discard the flow-through
- Transfer the column in new collection tube (2 ml)
- Add 500 µl RPE buffer, centrifuge for 15 s, maximum speed, discard the flow-through(centrifuge again for 2 min)
- Transfer the column to a RNase-free tube (1.5 ml), add 50 µl of RNase-free water to the membrane of the column, centrifuge for 1 min, maximum speed, collect the flow-through (repeat if needed)
- Measuring the quantity of RNA using the Nanodrop spectrophotometer (should be blanked with Nuclease-free water before measuring).

2.5.2 RNA integrity analysis

- Gel preparation: put 550 µl gel matrix into a spin filter, centrifuge at 1,500 g for 20 min at room temperature, aliquot 65 µl filtered gel into RNase-free microfuge tubes (store for 4 weeks maximum).
- Preparing the Gel-Dye Mix: allow the RNA 6000 Pico dye concentrate to equilibrate to room temperature for 30 min, vortex for 10 s, spin down and add 1 µl to 65 µl filtered gel, vortex and spin at 13,000 g, 10 min.
- Loading the Gel-Dye Mix, RNA 6000 Pico Conditioning Solution and Marker according to the supplier's instructions.
- Load the diluted ladder and samples.
- Vortex in the adapter supplied in the kit and run the chip under RNA test program in the Agilent 2100 bioanalyzer.

2.5.3 Reverse Transcription (RT)

RNA samples (1 µg) were reverse transcribed using the Reverse Transcription System (Table 5), before reaction, the RNA sample dissolved in RNase-free water was incubated at 70°C for 10 min.

Table 5: RT-PCR reaction system

Components	Volume for 1 sample (µl)
$MgCl_2$, 25 mM	4
10xRT buffer	2
dNTP mix, 10 mM	2
Ribonuclease inhibitor	0.5
Reverse-transcriptase (23 U/µl)	0.65 (15 U)
Random hexamer oligodeoxyribonucleotides	0.5
RNase-free water	10.35
Total volume	20

2.5.4 Primer design and gel electrophoresis

Primers were designed using Primer-Blast (http://www.ncbi.nlm.nih.gov/tools/primer-blast/) (Ye, Coulouris et al. 2012), followed by quality control applying melting curve and agarose gel electrophoresis analyses of the PCR products (primer nucleotide sequences are listed in Table 3). For separation of DNA by gel electrophoresis, use 100 ml 2.2% agarose in 1x Tris-acetate/EDTA (TAE) buffer with 0.1 µg/ml ethidium bromide (EtBr solution: 10 mg/ml) with 2x12 lane comb in media size gel chamber to cast the gel; remove comb(s) carefully after 0.5- 1 h (gel should have completely solidified); fill electrophoresis chamber with 1x TAE running buffer with 0.1 µg/ml EtBr (ca. 1 liter). After addition of 6x Loading Solution (Fermentas, Schwerte, Germany) PCR products were separated by applying 80 V for ca. 1.5 h. Gel documentation was done with BioRad gel documentation machine using UV transillumination.

2.5.5 Real-time polymerase chain reaction (PCR)

GAPDH and target gene expression in RNAs from RCC tissues were quantified with specific primers using the LightCycler FastStart DNA Master SYBR Green I kit in a LightCycler. Experiments were carried out according to the user instructions of the kit and run on the Light-Cycler using the following settings:

Denaturation	95°C	10 min	
3-step PCR:			
Denaturation	95°C	10 s	40 cycles
Annealing	60°C	10 s	
Extension	72°C	16 s	
Melting curve			
Cooling			

Crossing points (Cp) were used to calculate relative mRNA levels using the formula 2^{-Cp}. These values were normalized using the corresponding GAPDH mRNA levels of each sample. Normalized mean expression in normal tissues for each gene was used as a calibrator (expression set to 1).

2.6 Immunochemistry (IHC)

2.6.1 Preparation of tissue sections and cytospins

Tissue sections (10 µm) of tissues were prepared at -20°C using a Leica CM3050 microtome (Leica, Wetzlar, Germany), applied to Super Frost Ultra Plus® slides and stored at -20°C until used. Cytospins were prepared with the Cytospin 2 centrifuge (SHANDON, Frankfurt, Germany). Briefly, prepare a cell suspension of not more than $0.5x10^6$ cells/ml of serum-containing medium, prepare the slides mounted with the

paper pad and the cuvette in the metal holder, load up to 200 µl this suspension in each cuvette, then spin at 800 rpm for 3 min.

2.6.2 Staining procedure

For immunohistochemistry, BLOXALL Blocking Solution (Vector Laboratories, Inc. Burlingame, CA) was used for quenching of endogenous peroxidase after fixation with acetone for 5 min. Then frozen sections and cytospins were incubated with primary antibodies followed by detection using ImmPRESS Universal Reagent and ImmPACT Reagent kits (Vector Laboratories) according to the manufacturer's instructions. Then, tissue sections were counterstained using hematoxylin and covered for photography.

2.7 Western blotting

2.7.1 Preparation of materials and apparatus

Materials: Cell suspension or tissue samples, lysis buffer (50 mM Tris-HCl, 150 mM NaCl, 1% Triton X-100, pH=8.0), Complete Mini Protease Inhibitors Cocktail (Roche, Mannheim, Germany), ice bucket (big and small), cooled microcentrifuge (4°C), Nanodrop 2000 (Thermo Fisher Scientific, Barrington, USA), XCellSureLock Mini-Cell electrophoresis system (Invitrogen, NY, USA), NUPAGE Novex-Bis-Tris Gel (Invitrogen), Transfer buffer 20x (Invitrogen), MOPS SDS Running Buffer 20x (Invitrogen), 10 ml Syringe 23G 11/4 Nr. 14, distilled water, Dual Color Protein Marker (-20°C), 10% DTT (-20°C), 4x Loading buffer LDS, Thermoblock (set at 95°C), XCell II Blot Module (Invitrogen, NY, USA), Blotting milk buffer, Methanol, PDVF membrane 6x8 cm, Blotting pads, Parafilm, Electrophoresis gel, Trowel or "Blot-knife" (to open the Gel frames), Tweezer, Petri dishes, Ponceau dye solution, gloves, primary and

sencondary HRP-labeled antibodies, ECL Western Blotting System (GE, Freiburg, Germany), 100 ml 1x Washing buffer (T-PBS): 10 ml 10x PBS+90 ml dH_2O+100 µl Tween 20. A dark room with scissor, timers, red light, exposition portfolios, Hyperfilm™ ECL and development machine is needed for film development.

2.7.2 Procedure

Lysates of tissue cryosections from patients' tissues and cells were prepared in lysis buffer containing Complete Mini Protease Inhibitors Cocktail. Protein concentrations were measured using Nanodrop 2000 for further use. The same amount of protein (100 µg per lane) was separated by SDS polyacrylamide gel electrophoresis using the XCellSureLock Mini-Cell electrophoresis system and transferred to PDVF membranes using the Xcell II Blot Module. After blocking and antibody incubation of the membrane, the ECL Western Blotting System was used for visualization of bound antibodies.

2.8 Microarray data analysis (dChip and GSEA)

Probe preparation, hybridization and scanning of oligonucleotide microarrays (GeneChip HG U133 Plus 2.0, Affymetrix) was described before (Maruschke, Hakenberg et al. 2013). Briefly, Tissue samples were collected from RCC patients undergoing surgical resection of RCC. In total, there were 28 samples from primary tumor (14x grade G1, 14x grade G3), 14 samples from normal kidney tissue (tissue samples without macroscopic or microscopic alterations from tumor-bearing kidney) and 32 samples from metastases. All cases were clear-cell subtype of RCC. Patients did not receive systemic antitumoral treatment before surgery. All patients gave written informed consent, and the research was approved by the local ethics committees. Hybridization on oligonucleotide

microarrays (GeneChip HG U133 Plus 2.0, Affymetrix) was carried out overnight at 45°C using the Hybridization Oven 640 (Affymetrix) and Fluidics Station 450 (Affymetrix) following the standard protocols. Scanning of the microarrays was done using the GeneChip Scanner 3000 (Affymetrix), and raw data were stored as CEL files.

For calculation of the detection call ("absent" or "present") the Microarray Suite (MAS5) algorithm was used (software: Expression Console 1.1 from Affymetrix). The arrays were normalized and expression values were calculated using the dChip algorithm that is implemented in the software package dChip 2010 from http://www.dchip.org (Li and Wong 2001).

Gene set enrichment analysis (GSEA) (Subramanian, Tamayo et al. 2005) was used to determine the coordinate expression of a set of 46 EMT-associated genes which have been described to be up-regulated during EMT (Table 6). The GSEA software is available at http://www.broadinstitute.org/gsea for download. Briefly, GSEA compares gene expression in biological samples, e.g. primary tumor and normal tissue. Briefly, genes are ranked according to their signal-to-noise ratio (sum of the means of the gene in both groups divided by sum of the standard deviations). The algorithm calculates the running enrichment score (ES) by walking through the ranked list. The ES starts with zero, and it is increased each time when a gene is member of the gene set and decreased when it is not. The maximum deviation from zero is the final ES. When the genes of a gene set are enriched at one side of the ranked list (i.e., the majority is either up-regulated or down-regulated), then the final ES is high, indicating a meaningful up- or down-regulation of the gene set (pathway). The statistical significance (nominal P value) of the ES is calculated by using an empirical phenotype-based permutation test procedure. When an entire database of gene sets is evaluated, the estimated significance level is adjusted to account for multiple hypothesis testing.

2.9 Statistics

The unpaired two-tailed Mann-Whitney U test was used to compare gene expression levels between tumors of different stage and grade (TNMG classification). Statistical differences between transcript levels of normal kidney, primary tumor and metastases were analyzed using Kruskal-Wallis analyses with subsequent post-hoc tests. For survival analyses, the optimal cut-off value for each gene was determined using martingale residuals as described (Therneau 1990). Briefly, the martingale residual from a univariate Cox model exploring each gene was plotted on the y-axis against the respective gene expression value on the x-axis, and a smooth fit using the LOWESS (locally weighted scatterplot smoothing) function was calculated. The optimal cut-off was the expression value where the fitting line crossed zero on the y-axis. The low-risk and high-risk patient subgroups defined by this optimized cut-off value were further analyzed using univariate and multivariate methods. Outcome was evaluated using the Kaplan-Meier method and log-rank test. The starting point of follow-up was the time of surgery and the endpoint was cancer-specific survival. Additionally, multivariate Cox regression models were built which included mRNA expression levels of selected genes, TNM stage, and pathological tumor grade. Statistical calculations were performed using the software packages Prism 6.0 (GraphPad, San Diego, USA), R 2.15 (http://www.R-project.org/) and MedCalc 12.0 (MedCalc, Mariakerke, Belgium). $p<0.05$ was defined to be statistically significant.

3. Results

3.1 Microarray data analysis of EMT-related genes

3.1.1 Creation of EMT gene set list by database searching

By reviewing the former studies on EMT and solid tumors through PubMed searching, a gene list containing genes which were reported to be up-regulated in tumor undergoing EMT process was created. These genes encode adhesion molecules, transcription factors, chemokine receptors, metalloproteinases and others. The detailed gene list is shown in Table 6, genes are ranked by the enrichment score from highest to lowest obtained from gene set enrichment analysis.

Table 6: GSEA analysis of EMT-related genes and quantitative RT-PCR

Rank	Gene symbol	Probe set	Gene name (Alternative name)	Functional category (Gene Atlas)	Mean mRNA levels in normal kidney (n=14)	Mean mRNA levels in primary tumor (n=28)	Fold change primary tumor/normal (microarray)	Fold change primary (n=55)/ normal (n=19) (qRT-PCR)	Reference for role in EMT
1	VIM	201426_s_at	vimentin	structural protein	5815	14765	2.5	1.5	(Kalluri and Weinberg 2009, Zeisberg and Neilson 2009, Asiedu, Ingle et al. 2011)
2	SPARC	200665_s_at	secreted protein, acidic, cysteine-rich (osteonectin)	chaperone/stress , reg ulatory , structural protein , tumor suppressor	3649	9941	2.7	n.d.	(Asiedu, Ingle et al. 2011, Thomson, Petti et al. 2011)
3	CXCR4	217028_at	chemokine (C-X-C motif), receptor 4 (fusin)	receptor membrane G	491	4443	9.0	1.9	(Li, Ma et al. 2012)
4	TGFB1	203085_s_at	transforming growth factor, beta 1	regulatory , signaling growthfactor	319	1524	4.8	n.d.	(Kalluri and Neilson 2003, Thiery, Acloque et al. 2009, Asiedu, Ingle et al. 2011)
5	FN1	211719_x_at	fibronectin 1	adhesion	1586	8944	5.6	1.7	(Zeisberg and Neilson 2009, Asiedu, Ingle et al. 2011)
6	CXCR7	212977_at	chemokine (C-X-C motif) receptor 7	receptor membrane G	285	2530	8.9	3.3	(Asiedu, Ingle et al. 2011, Li, Ma et al. 2012)
7	TMEFF1	205122_at	transmembrane protein with EGF-like and two follistatin-like domains 1	tumor suppressor	32	145	4.6	n.d.	(Thomson, Petti et al. 2011)
8	ITGA5	201389_at	integrin, alpha 5 (fibronectin receptor, alpha polypeptide)	adhesion , receptor	297	1090	3.7	n.d.	(Kalluri and Weinberg 2009, Zeisberg and Neilson 2009, Asiedu, Ingle et al. 2011)
9	ETS1	224833_at	v-erythroblastosis virus E26 oncogene homolog 1 (avian)	transcription factor	1503	3656	2.4	n.d.	(Zeisberg and Neilson 2009)
10	TIMP1	201666_at	TIMP metallopeptidase inhibitor 1	enzyme	2833	9136	3.2	n.d.	(Asiedu, Ingle et al. 2011)
11	TCF4	203753_at	transcription factor 4 (E2-2)	transcription factor	568	1961	3.5	n.d.	(Thiery, Acloque et al. 2009)
12	SERPINH 1	207714_s_at	serpin peptidase inhibitor, clade H (heat shock protein 47), member 1, (collagen binding protein 1)	enzyme	477	1917	4.0	n.d.	(Zeisberg and Neilson 2009)
13	CDH2	203440_at	cadherin 2, type 1, N-cadherin (neuronal)	adhesion	1198	1988	1.7	9.1	(Thiery, Acloque et al. 2009, Zeisberg and Neilson 2009)
14	GNG11	204115_at	guanine nucleotide binding protein (G protein), gamma 11	receptor	2497	4617	1.8	n.d.	(Asiedu, Ingle et al. 2011)
15	MSN	200600_at	moesin	structural protein	3490	4931	1.4	n.d.	(Haynes, Srivastava et al. 2011)

Rank	Gene symbol	Probe set	Gene name (Alternative name)	Functional category (Gene Atlas)	Mean mRNA levels in normal kidney (n=14)	Mean mRNA levels in primary tumor (n=28)	Fold change primary tumor/normal (microarray)	Fold change primary (n=55)/ normal (n=19) (qRT-PCR)	Reference for role in EMT
16	CDH11	207173_x_at	cadherin 11, type 2, OB-cadherin (osteoblast)	adhesion	517	1508	2.9	n.d.	(Zeisberg and Neilson 2009)
17	COL3A1	201852_x_at	collagen, type III, alpha 1 (Ehlers-Danlos syndrome type IV, autosomal dominant)	structural protein	1630	4899	3.0	n.d.	(Asiedu, Ingle et al. 2011)
18	COL5A2	221729_at	collagen, type V, alpha 2	structural protein	158	1453	9.2	n.d.	(Asiedu, Ingle et al. 2011)
19	ITGAV	202351_at	integrin, alpha V (vitronectin receptor, alpha polypeptide, antigen CD51)	adhesion	3004	4612	1.5	n.d.	(Kalluri and Weinberg 2009, Zeisberg and Neilson 2009)
20	ACTA2	200974_at	actin, alpha 2, smooth muscle, aorta (α-SMA)	structural protein	3176	6606	2.1	n.d.	(Kalluri and Weinberg 2009, Zeisberg and Neilson 2009)
21	LAMA5	210150_s_at	laminin, alpha 5	adhesion	128	287	2.2	n.d.	(Zeisberg and Neilson 2009)
22	ZEB1	212764_at	zinc finger E-box binding homeobox 1; transcription factor 8 (represses interleukin 2 expression)	transcription factor	884	1507	1.7	13.8	(Liu, El-Naggar et al. 2008, Kalluri and Weinberg 2009, Zeisberg and Neilson 2009, Thomson, Petti et al. 2011)
23	FOXC2	214520_at	forkhead box C2 (MFH-1, mesenchyme forkhead 1)	transcription factor	21	29	1.4	n.d.	(Kalluri and Weinberg 2009, Zeisberg and Neilson 2009)
24	DES	202222_s_at	desmin	locomotion	108	163	1.5	n.d.	(Kalluri and Weinberg 2009)
25	PDGFRB	202273_at	platelet-derived growth factor receptor, beta polypeptide	receptor	273	641	2.3	n.d.	(Asiedu, Ingle et al. 2011)
26	TGFB2	228121_at	transforming growth factor, beta 2	signaling, cytokine growth factor	170	411	2.4	n.d.	(Kalluri and Weinberg 2009, Thiery, Acloque et al. 2009, Asiedu, Ingle et al. 2011)
27	CALD1	212077_at	caldesmon 1	structural protein	4492	6397	1.4	n.d.	(Thomson, Petti et al. 2011)
28	TCF3	210776_x_at	transcription factor 3 (E12/E47/E2A)	transcription factor	418	717	1.7	n.d.	(Kalluri and Weinberg 2009, Thiery, Acloque et al. 2009)
29	S100A4	203186_s_at	S100 calcium binding protein A4	regulatory	1018	2467	2.4	0.5	(Kalluri and Weinberg 2009, Zeisberg and Neilson 2009, Thomson, Petti et al. 2011)
30	COL1A2	202403_s_at	collagen, type I, alpha 2	structural protein	2071	5319	2.6	n.d.	(Kalluri and Weinberg 2009, Zeisberg and Neilson 2009, Asiedu, Ingle et al. 2011)
31	SERPINE1	202627_s_at	serpin peptidase inhibitor, clade E (nexin, plasminogen activator inhibitor type 1), member 1	enzyme	216	2342	10.8	n.d.	(Liu, El-Naggar et al. 2008, Asiedu, Ingle et al. 2011)

Rank	Gene symbol	Probe set	Gene name (Alternative name)	Functional category (Gene Atlas)	Mean mRNA levels in normal kidney (n=14)	Mean mRNA levels in primary tumor (n=28)	Fold change primary tumor/normal (microarray)	Fold change primary (n=55)/ normal (n=19) (qRT-PCR)	Reference for role in EMT
32	AHNAK	211986_at	AHNAK nucleoprotein (desmoyokin)	cell organization	3550	4708	1.3	n.d.	(Thomson, Petti et al. 2011)
33	LEF1	221558_s_at	lymphoid enhancer-binding factor 1	transcription factor	187	512	2.7	n.d.	(Thiery, Acloque et al. 2009, Zeisberg and Neilson 2009)
34	ZEB2	205063_at	zincfinger E-box binding homeobox 2 (SIP1, ZFHX1B)	transcription factor	111	260	2.3	0.8	(Kalluri and Weinberg 2009, Thiery, Acloque et al. 2009, Thomson, Petti et al. 2011)
35	MMP9	203936_s_at	matrix metallopeptidase 9 (gelatinase B, 92kDa gelatinase, 92kDa type IV collagenase)	enzyme	123	1166	9.5	1.0	(Kalluri and Weinberg 2009, Asiedu, Ingle et al. 2011)
36	TWIST1	213943_at	twist homolog 1 (acrocephalosyndactyly 3; Saethre-Chotzen syndrome) (Drosophila)	transcription factor	50	112	2.2	0.9	(Kalluri and Weinberg 2009, Zeisberg and Neilson 2009, Thomson, Petti et al. 2011)
37	DDR2	227561_at	discoidin domain receptor tyrosine kinase 2	regulation of cell proliferation	531	621	1.2	n.d.	(Kalluri and Weinberg 2009, Zeisberg and Neilson 2009)
38	CTNNB1	201533_at	catenin (cadherin-associated protein), beta 1, 88kDa	regulatory, signaling	2539	2929	1.2	n.d.	(Thiery, Acloque et al. 2009, Zeisberg and Neilson 2009, Thomson, Petti et al. 2011)
39	SNAI1	219480_at	snail homolog 1 (Drosophila)	transcription factor	119	154	1.3	n.d.	(Kalluri and Weinberg 2009, Thiery, Acloque et al. 2009, Zeisberg and Neilson 2009)
40	SNAI2	213139_at	snail homolog 2 (Drosophila)	transcription factor	424	576	1.4	0.6	(Kalluri and Weinberg 2009, Thiery, Acloque et al. 2009, Zeisberg and Neilson 2009)
41	MMP2	201069_at	matrix metallopeptidase 2 (gelatinase A, 72kDa gelatinase, 72kDa type IV collagenase)	enzyme	826	928	1.1	0.4	(Kalluri and Weinberg 2009)
42	MMP3	205828_at	matrix metallopeptidase 3 (stromelysin 1, progelatinase)	enzyme	14	14	1.0	n.d.	(Kalluri and Weinberg 2009)
43	GSC	1552338_at	goosecoid homeobox	transcriptionfactor	5	4	0.8	n.d.	(Kalluri and Weinberg 2009, Zeisberg and Neilson 2009)
44	FOXD3	241612_at	forkhead box D3	transcriptionfactor	18	9	0.5	n.d.	(Kalluri and Weinberg 2009)
45	IGFBP4	201508_at	insulin-like growth factor binding protein 4	signaling, cytokine growth factor	4919	3714	0.8	n.d.	(Thomson, Petti et al. 2011)
46	SDC1	201286_at	syndecan-1	structural protein , protooncogene, signaling	2747	1266	0.5	n.d.	(Zeisberg and Neilson 2009)

(END)

3.1.2 EMT genes are preferentially expressed in primary kidney tumors – Gene Set Enrichment Analysis (GSEA)

Raw data from previously described microarray study (Maruschke, Hakenberg et al. 2013) were used and included 42 samples from RCC patients (14 normal renal tissues from tumor-bearing kidneys, 14 G1 grade primary tumors, and 14 G3 grade primary tumors). GSEA was performed using the EMT gene set, a list of up-regulated genes in the process of EMT, to determine with confidence whether this set of functionally linked genes is coordinately up- or down-regulated between groups of biological samples.

GSEA in 28 primary tumors and 14 normal kidney tissues showed that expression of the EMT gene set was significantly enriched (up-regulated) in primary tumors compared to normal kidney tissues (false discovery rate (FDR)=0.01, nominal $p<0.05$; Figure 2A). Out of the 46 EMT gene set genes, 34 genes contributed to the core enrichment and exhibited on average 3.4-fold higher expression (range 1.3 to 10.8 fold) in RCC compared to normal kidney (Table 6). Among the top-ranked genes (those with a higher signal/noise ratio) were genes such as CXC chemokine receptor 4 (CXCR4; fold change (fc) = 9.0), CXCR7 (fc=8.9), fibronectin (FN1; fc=5.6), transforming growth factor ß1 (TFGB1; fc=4.8) and vimentin (VIM; fc=2.5) with well-defined functions in EMT and tumor stem cell biology. In contrast, comparison between G1 and G3 grade primary tumors did not reveal significant differences (FDR=0.84, Figure 2B).

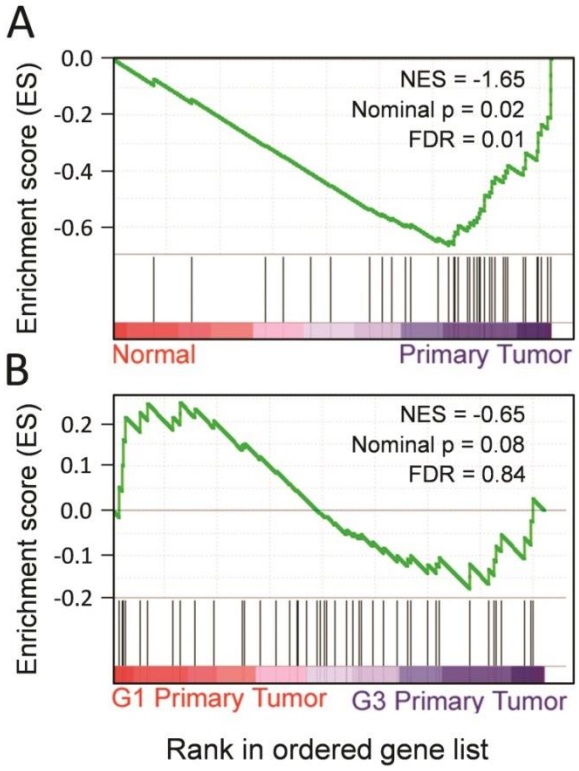

Figure 2: Gene set enrichment analysis (GSEA) of EMT-associated genes in RCC. Genes were ranked according to their differential expression between (A) normal kidney (n=14) and primary RCC (n=28) and (B) G1 primary RCC (n=14) and G3 primary RCC (n=14). Expression levels were determined by oligonucleotide microarray analysis. Red bars indicate genes expressed preferentially in normal tissues and G1 primary tumors, blue bars genes overexpressed in primary tumors and G3 primary tumors with color intensity corresponding to the degree of overexpression (dark > light). Black bars below the graph mark the position of the set of 46 genes up-regulated during EMT. Significant enrichment of this gene set was observed with the majority of the genes being higher expressed in primary tumors than in normal kidney (FDR 0.012); no enrichment was seen for the G1/G3 primary tumor comparison (FDR 0.844). ES, enrichment score; FDR, false discovery rate; NES, normalized enrichment score.

3.1.3 Expression pattern of EMT-related genes in different groups of samples – microarray analysis

Normalized genome-wide gene expression data were further analyzed using dChip. The overall expression pattern of EMT genes is shown as heat map in Figure 3 created by GSEA (listed from top to bottom are the least to the most up-regulated genes in primary tumor).

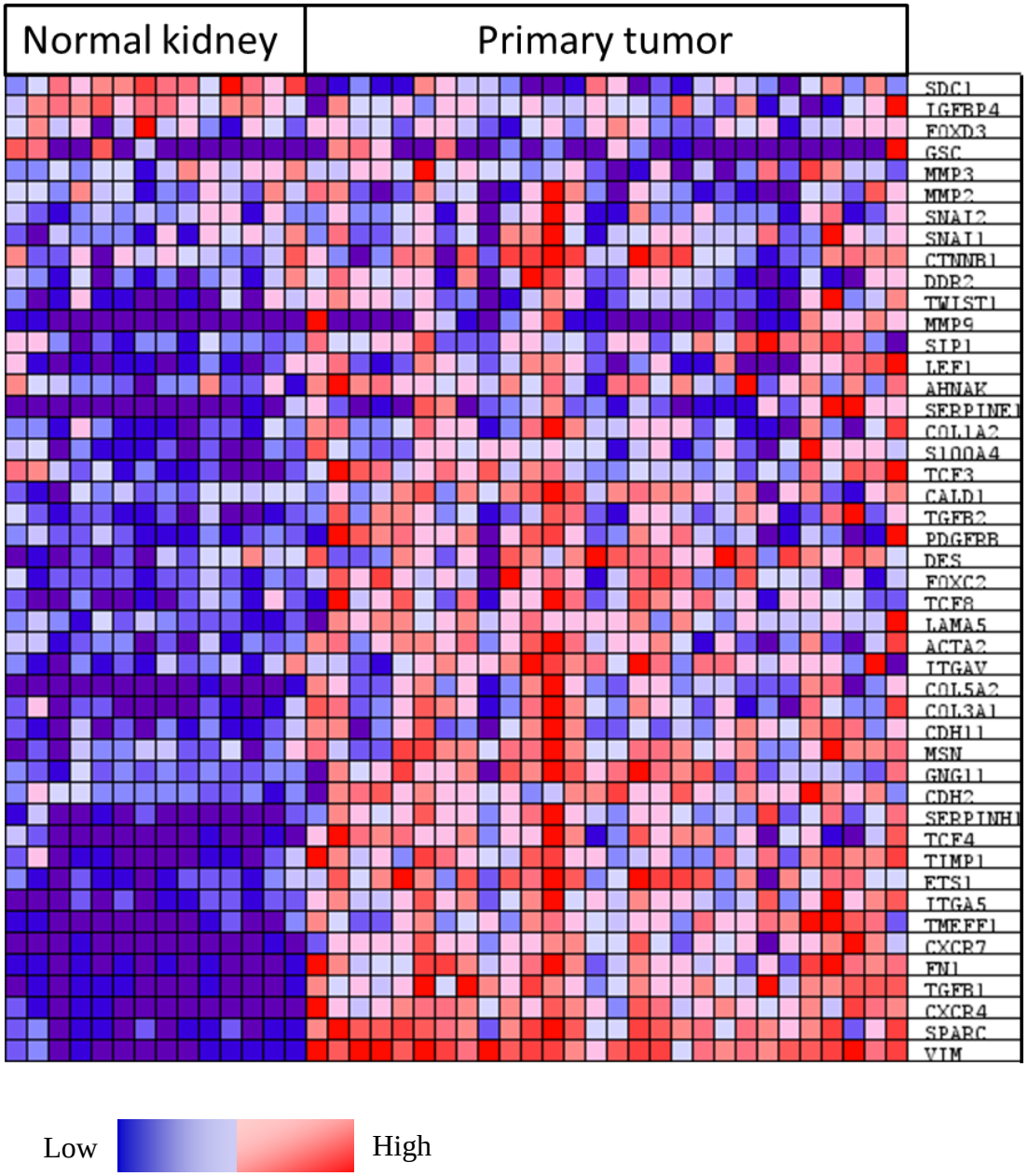

Figure 3: Heat Map by GSEA. Gene expression of each gene from EMT-related gene list is shown (14 normal kidneys and 28 primary tumors). Red: up-regulation, blue: down-regulation.

Comparison of the expression levels of individual genes in normal kidney tissue and primary tumor as well as in G1 and G3 grade primary tumors are shown in Figure 4: *FN1, ITGA5, LEF1, MMP9, S100A4, SERPINE1, TGFB1* and *TIMP1* represent higher expression in primary tumor compared to normal kidney, while gene expression in G3 primary tumors is higher than that in G1 primary tumors (Figure 4A-H). *CDH1*, encoding E-cadherin, has an opposite expression pattern as the eight genes (Figure

4I).Additionally to the 8 of 46 genes mentioned above, another 27 genes have also significantly increased expression in overall primary tumors (G1/G3) compared to normal kidney tissues while no significant difference between G1 and G3 grade tumors was found (Figure 5, shown in two separated parts).

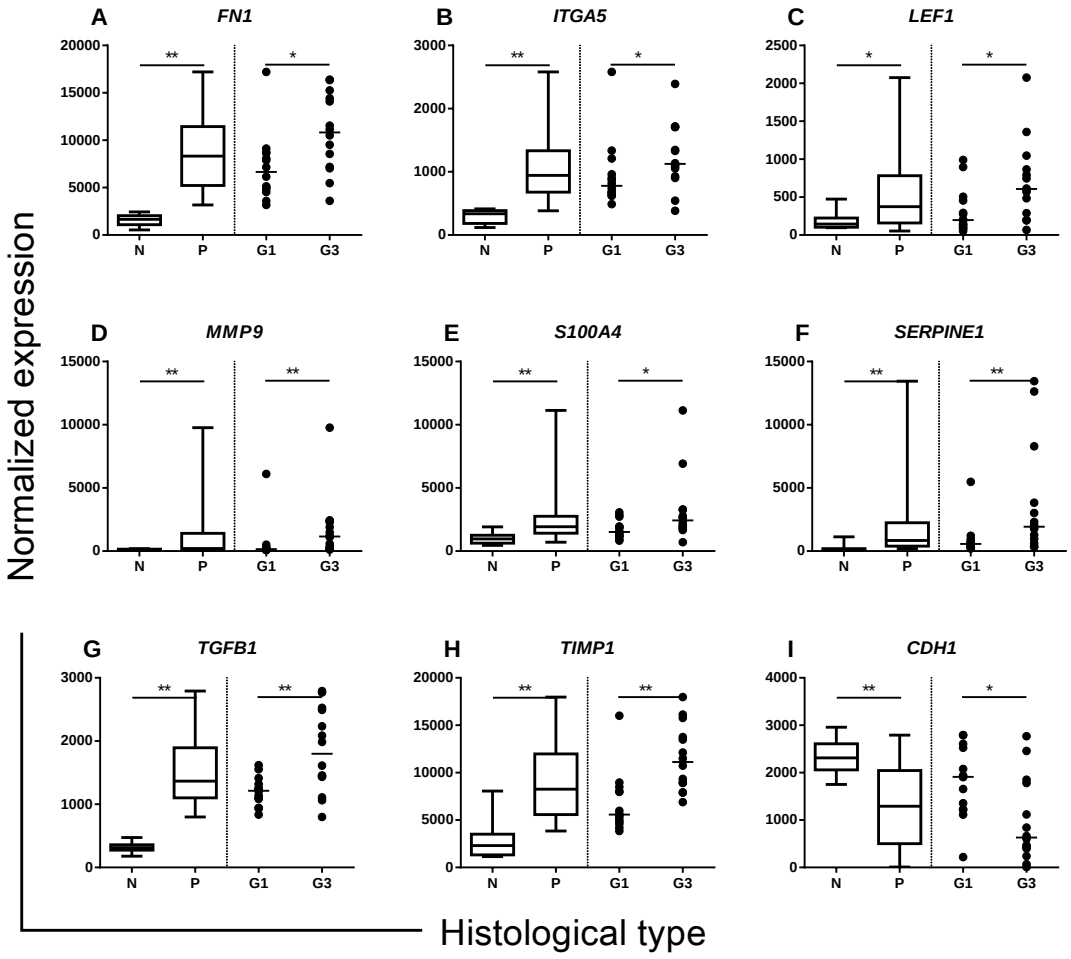

Figure 4: Box plots of genes with significantly increased expression in primary tumors compared to normal kidney, and increased expression in G3 grade primary tumors compared to G1 grade tumors. The results are shown as box plots with median and 25 and 75 percentiles or as dot plots. Whiskers mark the maximum and minimum values. *P* values below the graphs indicate the overall statistical significance determined by Kruskal-Wallis analyses. Individual statistical significance is depicted by brackets and asterisks. *, $p<0.05$; **, $p<0.01$. N, normal renal tissue from tumor-bearing kidney; P, primary tumor; M, metastases; G1/G3, tumor grade.

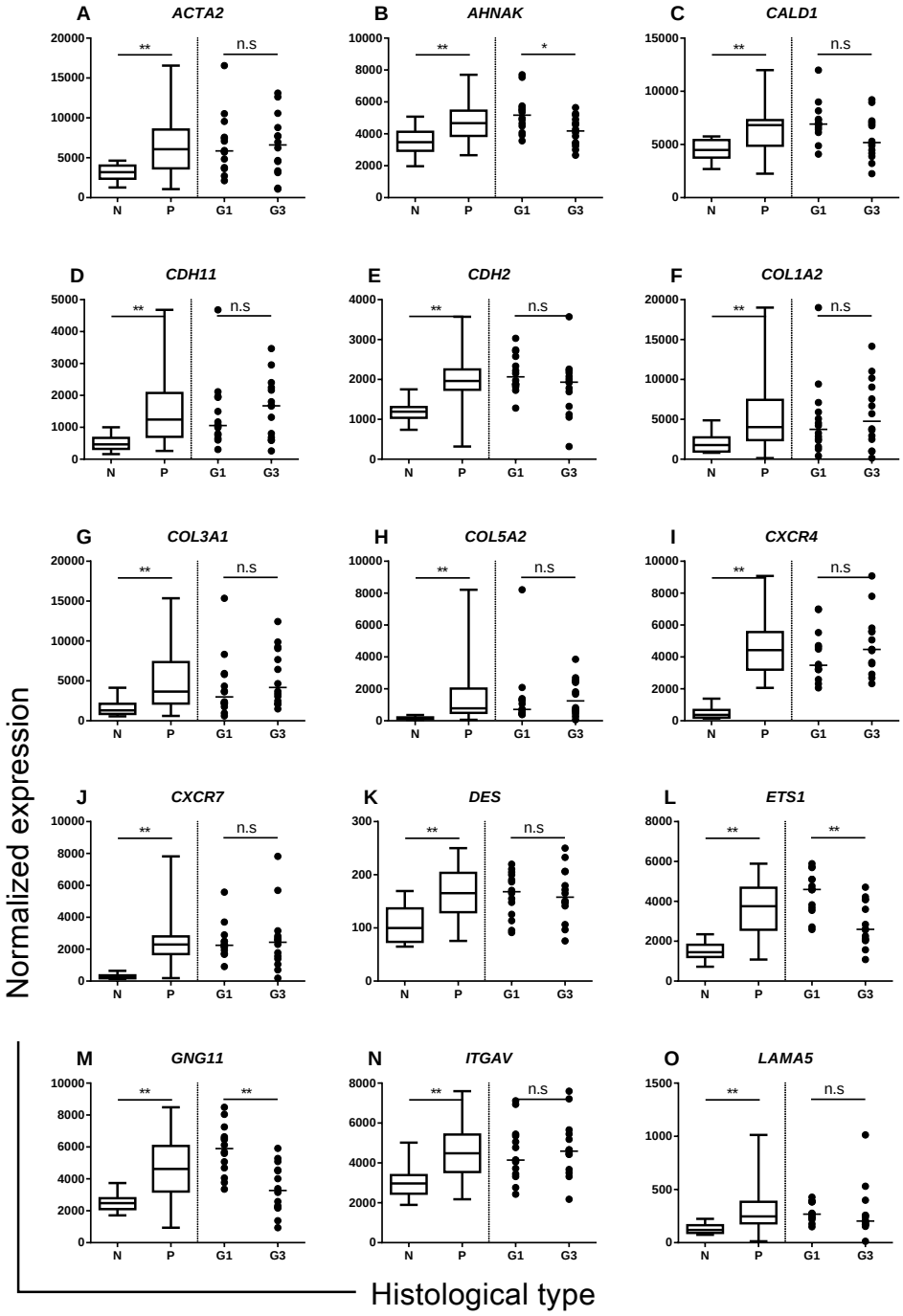

Figure 5 (part I): Box-plots of genes which have significantly increased expression in primary tumors compared to normal kidney, but have no significantly increased expression in G3 primary tumors compared to G1 primary tumors. The results are shown as box plots with median and 25 and 75 percentiles or as dot plots. Whiskers mark the maximum and minimum values. *P* values below the graphs indicate the overall statistical significance determined by Kruskal-Wallis analyses. Individual statistical significance is depicted by brackets and asterisks. *, $p<0.05$; **, $p<0.01$. N, normal renal tissue from tumor-bearing kidney; P, primary tumor; M, metastases; G1/G3, tumor grade.

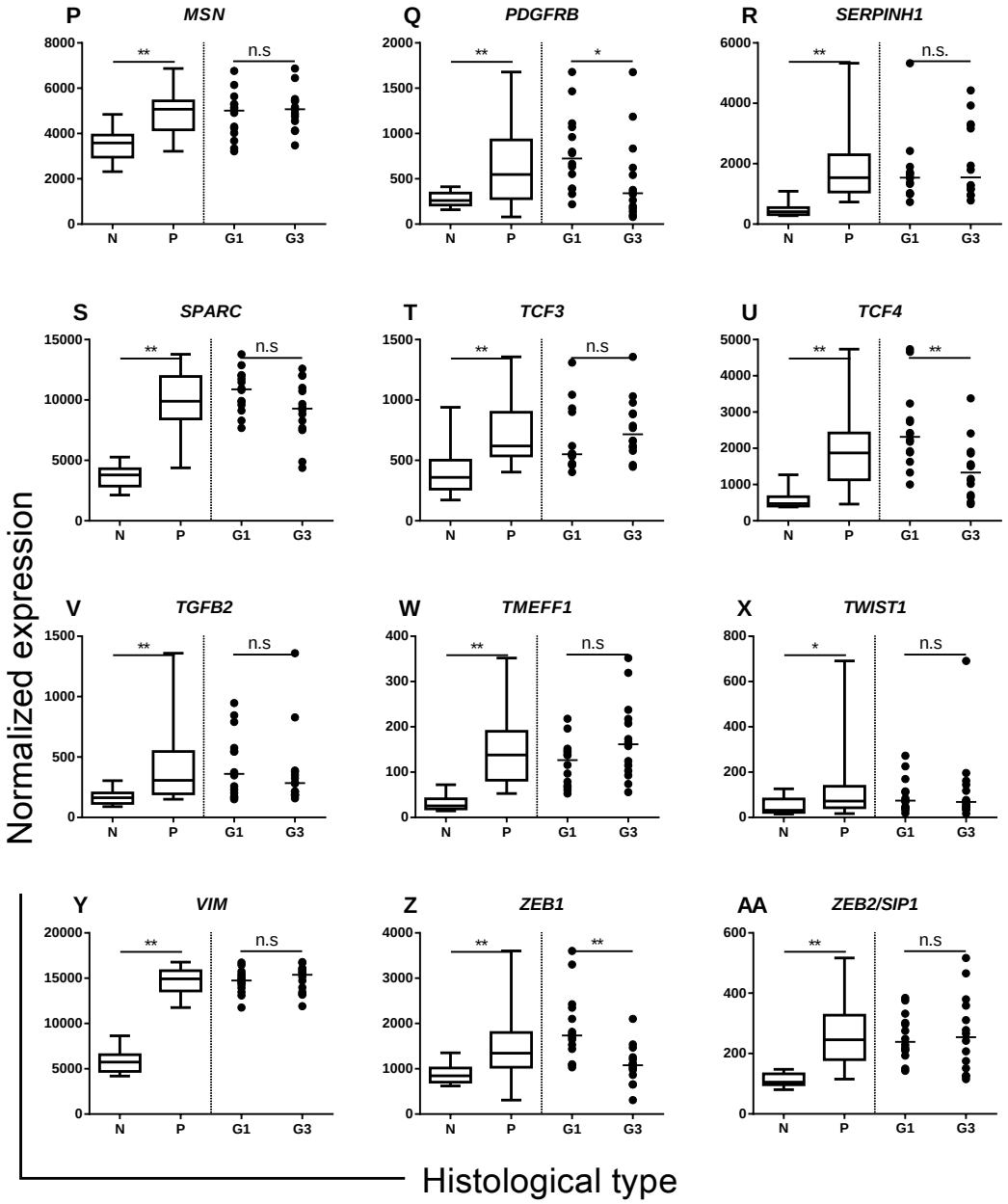

Figure 5 (part II): Box-plots of genes which have significant increased expression in primary tumors compared to normal kidney, but have no significantly increased expression in G3 primary tumors compared to G1 primary tumors. The results are shown as box plots with median and 25 and 75 percentiles or as dot plots. Whiskers mark the maximum and minimum values. *P* values below the graphs indicate the overall statistical significance determined by Kruskal-Wallis analyses. Individual statistical significance is depicted by brackets and asterisks. *, $p<0.05$; **, $p<0.01$. N, normal renal tissue from tumor-bearing kidney; P, primary tumor; M, metastases; G1/G3, tumor grade.

3.1.4 Prognostic significance of EMT-related gene expression in RCC patients based on microarray data

For each gene, Kaplan-Meier curves were drawn to evaluate the predictive power of EMT-related genes in patient outcome. In primary tumors, correlation of gene expression and patient outcome was analyzed and genes that have a potential predictive role are shown in Figure 6 (genes are ranked from smallest to largest *p* value, genes with a $p<0.20$ are shown).

To test whether transcript levels of additional EMT-associated genes could potentially serve as outcome predictors, we correlated mRNA levels of the 46 EMT-related genes of the set of primary tumors (n=28) used for transcriptome analysis with tumor-specific survival. Higher mRNA levels of 7 of the genes investigated correlated significantly with poor survival (*TGFB1)*, serpin peptidase inhibitor (*SERPINE1*), integrin α5 (*ITGA5*), transcription factor 3 (*TCF3*), *FN1*, *MMP9*, TIMP metallopeptidase inhibitor 1 (*TIMP1*); *p* between 0.001 and 0.020. Higher *CDH1* transcript levels predicted significant better outcome ($p=0.009$; Figure 6A-H). Another subset of 7 mRNAs including *VIM* and *MMP2* transcripts exhibited *p* values between 0.05 and 0.18 (Figure 6I-O).

In summary, lower expression of CDH1 and higher expression of *TGFB1, SERPINE1, ITGA5, TCF3, FN1, MMP9* and *TIMP1* predict poor outcome of RCC patients in univariate survival analysis.

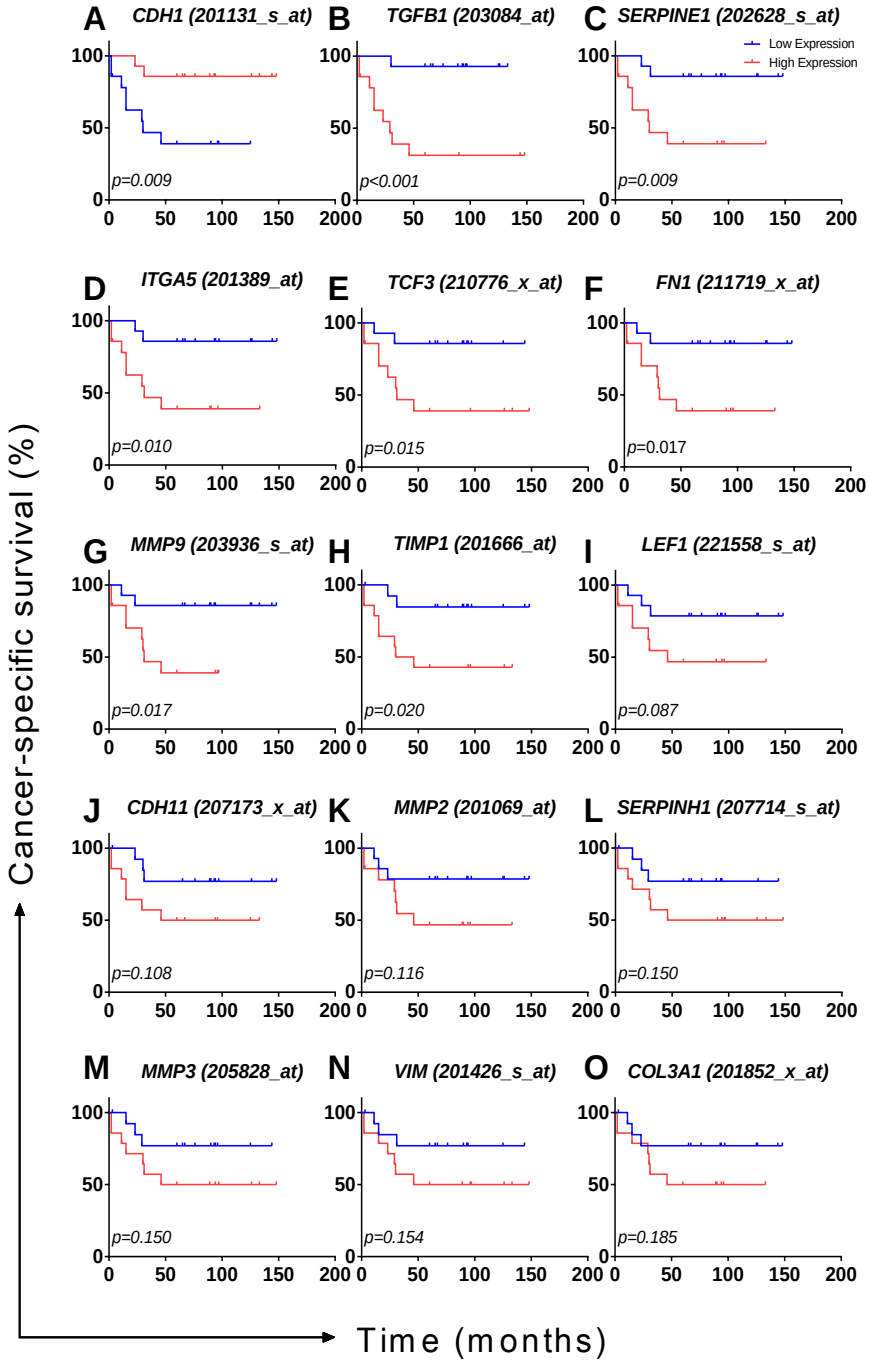

Figure 6: Kaplan-Meier survival analysis of RCC patients based on EMT-related gene expression determined by transcriptome analyses in primary tumor samples. Oligonucleotide microarray expression data from primary tumors of a total of 28 patients for the set of 46 EMT-associated genes and cancer-specific survival time were used for calculation (10 deaths occurred during the observation period). Cancer-specific death is used as endpoint. Median mRNA levels were used as cut-off. Low mRNA level groups are represented as blue (low expression), high level groups as red curves (high expression). *P* values for each gene are included in the graphs. Results are only shown for $p<0.2$. *p* value <0.05 were considered significant.

3.2 PCR validation of selected genes

3.2.1 Expression of selected genes

To validate differential expression of EMT-related genes in normal renal tissues and primary RCC and to determine whether these genes are similarly deregulated in metastases, we performed quantitative PCR analyses using RNA from normal renal tissue, primary tumors and metastases from an independent cohort of RCC patients. We selected a subset of the EMT-related genes which were found to be among the top ranked genes in the GSEA analysis or are known to represent master transcriptional regulators in other tumor entities or have been shown to be functionally important for tumor progression like extracellular matrix-degrading metalloproteinase (Table 6) as well as *CDH1,* the down-regulation of which is considered a hallmark of EMT(De Craene and Berx 2013).

Five out of the 13 analyzed genes i.e. *CXCR4*, *CXCR7*, *VIM*, *CDH2* (encoding N-cadherin) and *ZEB1* (*zinc finger E-box binding homeobox 1*) were up-regulated in primary RCC compared to normal tissue (Figure 7A-F). In metastases, even higher median mRNA levels were found for *VIM*, *CXCR4* and *FN1* (Figure 7A, B, D). Interestingly, compared to primary tumors lower mRNA levels were observed in metastases for *CXCR7, ZEB1* and *CDH2* (p<0.001, Figure 7C, E, F). These findings could indicate reversal of EMT during metastasis. CDH1 was down-regulated in primary tumors and metastases compared to normal kidney tissues.

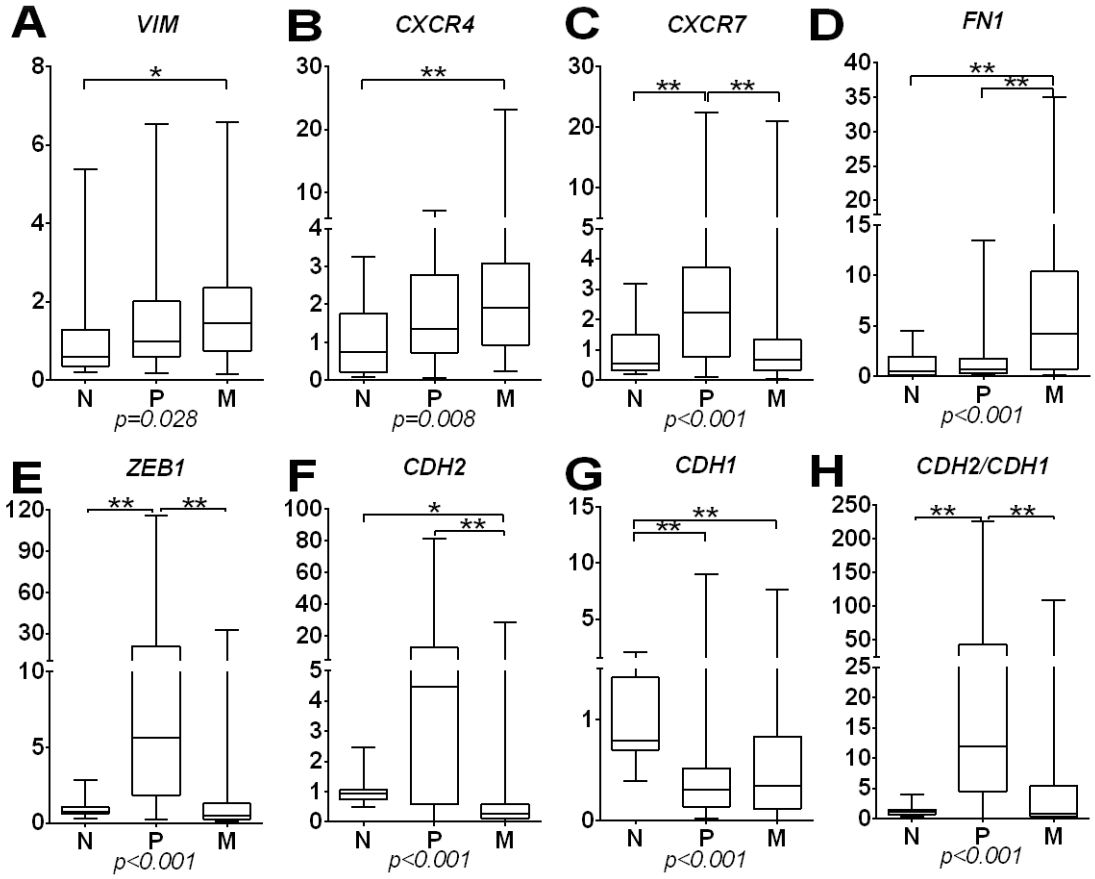

Figure 7: EMT-associated gene expression during RCC progression. (A-G) Normalized transcript levels of the indicated genes were determined by real-time PCR after reverse transcription of total RNA from normal renal tissue from tumor-bearing kidney (N), primary tumor (P) and metastases (M). The mean value of normalized expression in normal tissue was used as the calibrator (set to 1). To identify a potential cadherin switch, the ratio of CDH2/CDH1 mRNA content was calculated for each sample (H). The results are shown as box plots with median and 25 and 75 percentiles. Whiskers mark the maximum and minimum values. *P* values below the graphs indicate the overall statistical significance determined by Kruskal-Wallis analyses. Individual statistical significance is depicted by brackets and asterisks. *, $p<0.05$; **, $p<0.01$.

3.2.2 Cadherin switch is observed in primary tumors and reversed in metastases

Loss of *CDH1* expression resulting in disruption of tight junctions and concomitant gain of cell motility is typically observed during EMT. Another characteristic feature of the EMT process is increased expression of the cell adhesion molecule N-cadherin (encoded by *CDH2*) which is often observed in parallel. This inverse regulation of expression of *CDH1* and *CDH2* is referred to as cadherin switch (Gravdal, Halvorsen et al. 2007). We found that *CDH1* had on average lower expression levels both in primary RCC tumors and metastases compared to normal tissue ($p<0.01$), while *CDH2* was up-regulated in primary tumors compared to normal tissue and down-regulated in metastases compared to primary tumors (Figure 6F, G). For each tissue sample, the ratio of CDH2/CDH1 mRNA levels was calculated. The ratio in primary tumors was significantly higher than in normal kidney samples ($p<0.01$, Figure 6H). In metastases, the ratio was significantly lower compared to primary tumors ($p<0.01$, Figure 6H).

3.2.3 Prediction of patient outcome based on EMT-associated genes expression

3.2.3.1 Kaplan-Meier analysis (univariate analysis)

For 49 out of 55 patients follow-up data were available and were used for survival analysis. The Kaplan-Meier analyses revealed that higher mRNA expression levels of *VIM*, *CXCR4* (both $p<0.001$), *FN1* ($p=0.02$) and *TWIST1* ($p=0.037$) in primary RCC were associated with a worse outcome (Figure 8A-D). Increased MMP2 mRNA levels were also associated with a worse outcome, but the differences were not significant ($p=0.101$; Figure 8F).

3.2.3.2 Multivariate Cox regression model

A multivariate Cox regression model was established using prognostic factors such as TNM stage, pathological grade and mRNA levels of selected genes. The multivariate analysis was carried out with data from 44 patients with complete datasets because in some patients the presence of lymph node metastases was unknown (pNX). Up-regulation of CXCR4 and VIM mRNA in primary tumors were independent prognostic markers (p=0.042 and p=0.008, respectively) for an unfavorable outcome in RCC patients (Table 7).

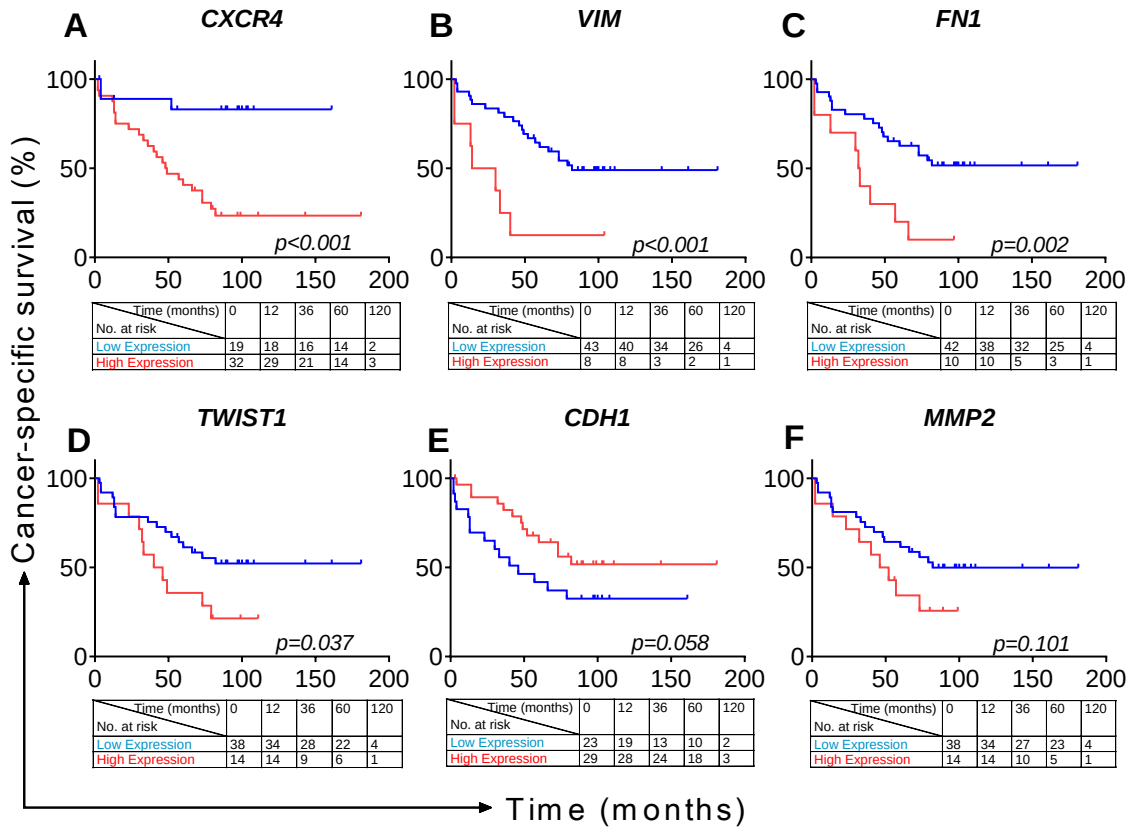

Figure 8: Kaplan-Meier survival analysis of RCC patients based on EMT-related gene expression determined by RT-PCR in primary tumor samples. Expression data from primary tumors of a total of 49 patients and cancer-specific survival time were used for calculation (28 deaths occurred during observation period). Cancer-specific death is used as endpoint. Low mRNA level groups are represented as blue, high level groups as red curves. Patients at risk at 0, 12, 36, 60 and 120 months after surgery are shown below the graphs. *P* values for each gene are included in the graphs. $p<0.05$ were considered significant. Genes with a $p \leq 0.1$ are shown.

Table 7: Determination of prognostic power of pathological and clinical parameters and EMT gene mRNA levels in primary tumor by multivariate Cox regression analysis

	Hazard ratio	95% confidence interval	*p* value*†
T1-2 vs.T3-4	1.5	0.5 – 4.4	0.483
N0 vs. N+	1.1	0.3 – 3.7	0.929
M0 vs. M1	5.2	1.7 – 16.1	**0.004**
G1-2 vs. G3	0.6	0.2 – 2.2	0.436
VIM low vs. high	7.6	1.7 – 34.4	**0.008**
CXCR4 low vs. high	3.8	1.1 – 13.9	**0.042**

* 44 patients, 23 events during follow-up; endpoint: tumor-specific survival, †*p* values < 0.05 are shown in **bold**

3.3 Expression and prognostic value of TPBG and CXCR4 in RCC

CXCR4 was shown above to be an independent prognosis marker and proven by our group as a stem cell marker in renal cell carcinoma (Gassenmaier, Chen et al. 2013). The overexpression of CXCR4 was found to be correlated with metastasis, migration, cell renewal and proliferation (Domanska, Kruizinga et al. 2013). Two other molecules, CXCL12 and TPBG, are important for CXCR4 function. CXCL12 is known as ligand of CXCR4, while TPBG, also named 5T4, was reported to be critical for the surface expression of CXCR4.

3.3.1 Expression of CXCR4 in RCC

So far, expression of CXCR4 has only been analyzed at the mRNA level. In order to prove the presence of CXCR4 protein, immunohistochemistry and Western blot analyses were carried out using either tissue samples from patients or cytospins. HEK-293T cells transfected with a CXCR4 expression plasmid and un-transfected HEK-293T cells served as positive and negative controls, respectively. Staining with an anti-CXCR4 antibody revealed that CXCR4-transfected HEK-293T cells had a high proportion of positive cells while the un-transfected cells were totally negative after

staining (Figure 9A, B). In general, a higher number of CXCR4-positive cells were observed in primary tumors and metastases compared to normal kidney tissues (Figure 9C-E). Furthermore, CXCR4 expression was found to agree well at the mRNA and protein level as determined by real-time PCR and Western blot, respectively (Figure 9F, G).

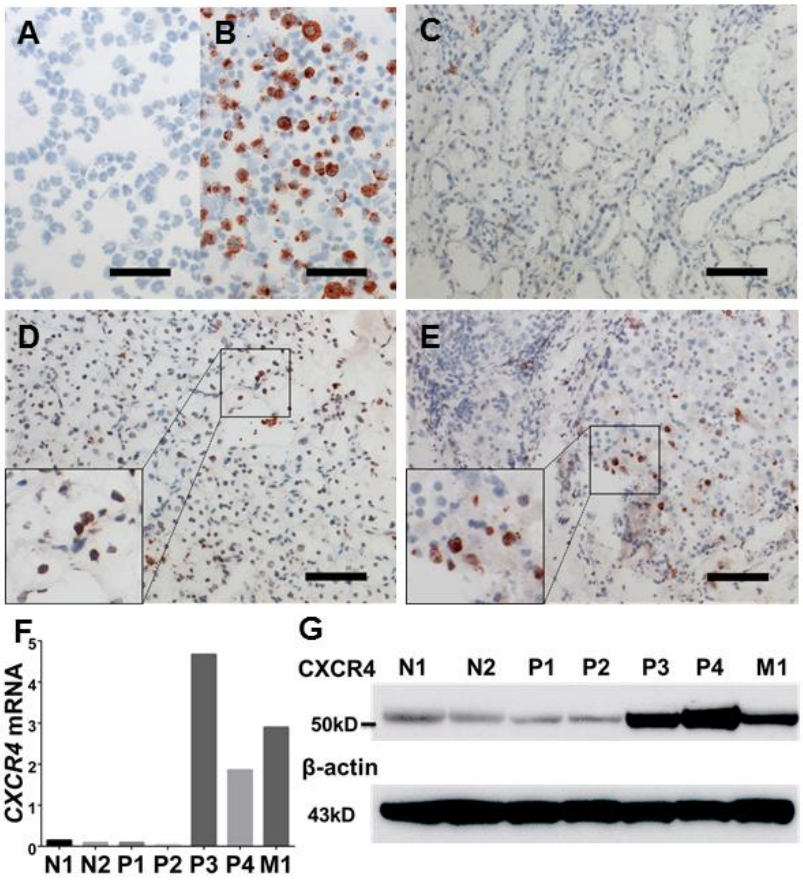

Figure 9: Correlation of CXCR4 mRNA and protein levels in cell lines, normal kidney and RCC tissues: Immunohistochemistry staining of CXCR4 in (A) HEK-293T cells, (B) *CXCR4*-transfected HEK-293T cells, (C) normal kidney, (D) primary tumor and (E) RCC lung metastasis; *GAPDH*-normalized expression of *CXCR4* as determined by real-time PCR (F); Western Blot detection of CXCR4 (G): Normal tissue (N1 and N2), primary tumors with low CXCR4 expression (P1 and P2), primary tumors with high CXCR4 expression (P3 and P4), and metastasis (M1). Scale bar=200 µm.

3.3.2 Expression and prognostic significance of TPBG in RCC

Expression of TPBG was also measured by real-time PCR and IHC. Expressions of TPBG in primary tumors are higher than that in normal kidney samples and metastases (Figure 10A, overall $p<0.001$). Two primary tumor samples were excluded from expression and survival analysis because they were clearly defined as outliers regarding the expression of TPBG. Lower TPBG mRNA level indicate a better outcome of RCC patients (Figure 10B, $p=0.036$). TPBG expression level was an independent prognostic marker in RCC patients according to Cox regression model (Table 8, $p=0.037$).

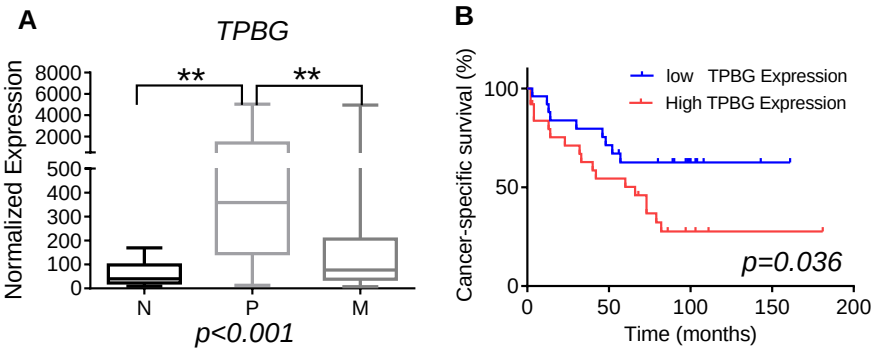

Figure 10: Expression and prognostic significance of TPBG in RCC patients. (A) mRNA expression of TPBG determined by real-time PCR in 19 normal kidney tissues (N), 50 primary tumors (P) and 38 metastases (M); (B) TPBG expression correlates with patient outcome (Kaplan-Meier analysis). Median expression was used as cut-off of high/low expression.

Table 8: Multivariate analysis of TPBG expression with TNM stage and pathological grade (Cox regression model)

Covariate	Hazard ratio	95% confidence interval	*p* value*†
T1-2 vs.T3-4	0.8	0.3-2.3	0.742
N0 vs. N+	2.3	0.9-6.0	0.100
M0 vs. M1	3.2	1.0-9.8	**0.042**
G1-2 vs. G3	2.2	0.8-5.9	0.120
TPBG low vs. high	2.7	1.1-6.8	**0.037**

* 44 patients, 23 events during follow-up; †*p* values < 0.05 are shown in bold

3.3.3 RCC cell lines do not coexpress CXCR4 and TPBG

HEK-293T cells were transfected with expression plasmid of CXCR4 and TPBG to verify the specificity of fluorescent antibodies used. The gating strategy is shown in Figure 11. Un-transfected HEK293T cells were taken for example.

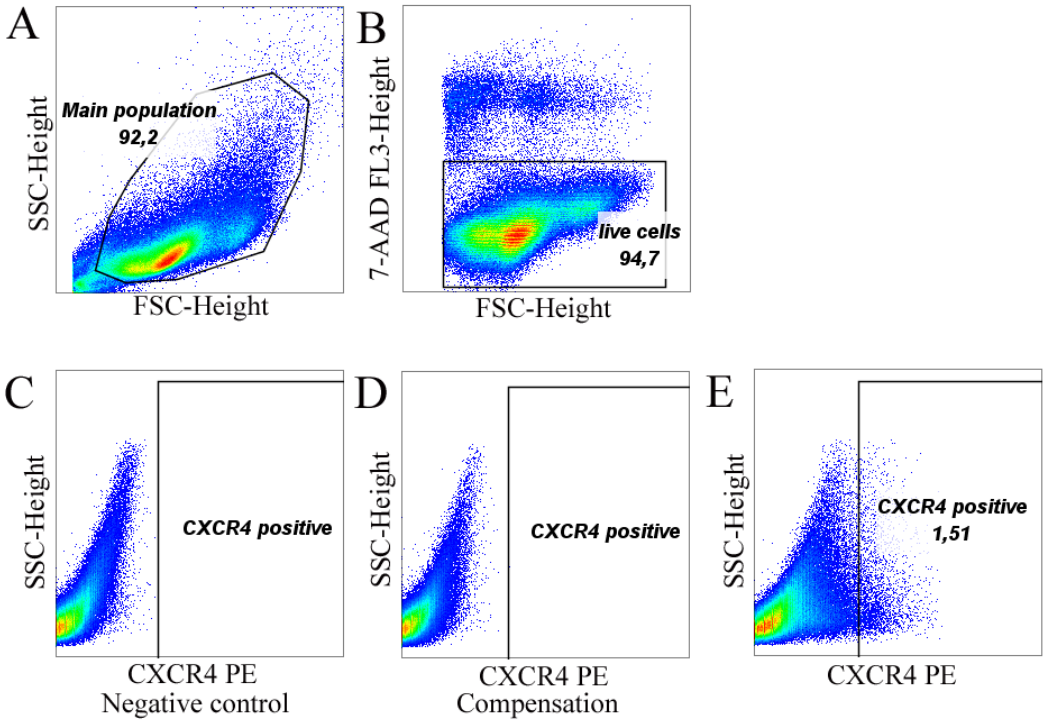

Figure 11: Gating strategy for transfected and untransfected HEK-293T cells. (A) Firstly, the main population is gated in a FSC-H vs. SSC-H plot to exclude debris located in the lower left corner; (B) in a FSC-H vs. FL3-H plot, 7-AAD-positive cells (high fluorescence FL3; dead cells) are excluded; (C) the negative control HEK-293T cells (no anti-CXCR4 or anti-TPBG antibodies) were used to exclude the influence of auto-fluorescence of cells; (D) compensation: single stained control HEK-293T cells were used to avoid potential interfere of fluorescence of APC-conjugated anti-TPBG antibodies (FL4); (E) the percentage of HEK-293T cells positively stained for CXCR4 in CXCR4/TPBG double-stained cells. The unit for proportion in the figure is percentage (%).

CXCR4-transfected HEK-293T cells have a highly increased proportion of CXCR4-positive cells in comparison with un-transfected HEK-293T cells

(from 1.5% to 76.6%). TPBG-transfected HEK-293T cells also have an obviously higher proportion of TPBG-positive cells than un-transfected HEK-293T cells (Figure 12A, B).

After verifying the specificity of antibodies, SK-RC-17 and RCC53 cell lines were stained by APC-conjugated anti-TPBG and PE-conjugated anti-CXCR4 antibodies to investigate the potential co-localization of the two molecules on the cell surface. However, very low proportions of cells in both cell lines are double positive and no obvious sub-population of double-positive cells was found (Figure 12C, D).

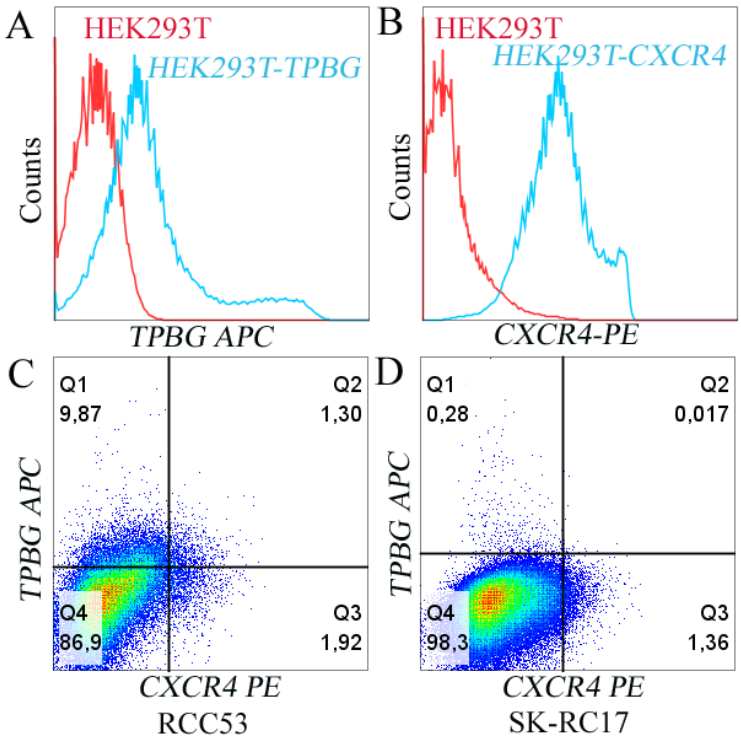

Figure 12: Antibodies specificity verification and double staining of TPBG and CXCR4 in RCC cell lines. Un-transfected HEK293T cells and TPBG (A) or CXCR4 transfected HEK293T cells (B) were counted by flow cytometry; double-stained renal cell carcinoma cell line RCC53 (C) and SK-RC-17 (D). The number of cells in each quadrant is indicated as percentage of total viable cells.

3.4 Genes consecutively higher expressed during tumor progression can predict survival

Analysis of microarray expression data from normal kidney, primary tumors and metastases revealed that for 59 probe sets (genes) there was increased expression in primary RCC compared with normal kidney, and at the same time in metastases compared with primary tumors (criteria: 2-fold difference each and $p<0.05$). In uni- or multivariate survival analysis, increased expression of 15 of these probe sets was significant. Undefined genes (C1orf216 and Hs.133294.1) and genes with very low mRNA level in RT-PCR (NDC80, GOLSYN, DTL, and BUB1B) were excluded. Eight genes (TOP2A, SFN, CENPF, AMPD3, ATAD2, AURKA, HELLS and TET3) were validated by quantitative RT-PCR. Multivariate survival analysis in an independent validation cohort of 52 primary RCCs showed that TOP2A (HR=4.4, $p=0.004$), TET3 (HR=2.9, $p=0.031$), HELLS (HR=3.6, $p=0.007$), and ATAD2 (HR=3.8, $p=0.014$) represent independent prognostic predictors for RCC patients.

4. Discussion

4.1 EMT takes place in RCC

Changes of cell morphology and the state of cell differentiation play an important role in embryogenesis and carcinogenesis (Boyer, Tucker et al. 1988, Thiery, Boyer et al. 1988). The conversions of epithelial cells to mesenchymal cells, named EMT, are commonly found in epithelial-origin carcinoma such as breast cancer (Yang, Liu et al. 2013), lung cancer (Zhang, Liu et al. 2013), gastrointestinal cancer (Teixido, Mares et al. 2013, Xia, Ooi et al. 2013, Zhao, Li et al. 2013, Zhu, Gao et al. 2013), squamous cell carcinoma (Yang, Chang et al. 2007), ovarian cancer (Ahmed, Abubaker et al. 2010), cervical cancer (Yan, Wang et al. 2013) and urological cancers (Wang, Fang et al. 2013, Zhu, Zhu et al. 2013). Since there is almost no knowledge so far about the role of EMT in RCC and about its impact on patients' prognosis, 46 EMT-related genes were selected from the literature and analyzed in RCC patients in this study.

By analyzing oligonucleotide microarray data using GSEA, 34 genes from a set of 46 genes known to be up-regulated during the EMT process were found to be significantly enriched in RCC compared to normal renal tissue, indicating an important role of EMT in RCC. Out of the 46 genes, 42 genes exhibited increased mRNA levels in primary RCC compared to normal kidney tissue with 26 genes showing a change larger than 2-fold (Table 6). Up-regulation of gene expression could be confirmed by RT-PCR for 5 out of 12 genes which were selected for validation in an independent cohort of RCC patients (Figure 7). This is further supported by the switch from E-cadherin to N-cadherin expression between normal kidney and primary RCC which is characteristic for EMT (Gravdal, Halvorsen et al. 2007).

TWIST (an activator of *CDH2* which encodes N-cadherin), SNAIL2 (also known as SLUG, a repressor of *CDH1* encoding E-cadherin) and the extracellular proteases matrix metalloproteinase 2 (MMP2) and 9 (MMP9) are classical EMT markers and serve as effectors of EMT. Increased expression of *MMP2* and *MMP9* was verified in renal cell carcinoma to be correlated with poor prognosis (Kallakury, Karikehalli et al. 2001). Zinc finger E-box binding homeobox 1 (ZEB1) and 2 (ZEB2) are proposed to be EMT-activators functioning as transcriptional repressors of E-cadherin expression (Aigner, Dampier et al. 2007). S100A4/FSP1 is known as a facilitator of EMT and is used as a marker for epithelial cells undergoing early-stage EMT (Okada, Danoff et al. 1997, Teng, Zeisberg et al. 2007). The prognostic significance of *S100A4* expression was demonstrated for human breast cancer and renal cell carcinoma (Rudland, Platt-Higgins et al. 2000, Bandiera, Melloni et al. 2009). CXC chemokine receptor 4 (CXCR4) is recognized as an stem cell marker in renal cell carcinoma (Gassenmaier, Chen et al. 2013), the role of CXCR4 signaling in tumor invasion and metastases was proved in lung cancer, pancreatic cancer and also in renal cell carcinoma (Pan, Mestas et al. 2006, D'Alterio, Barbieri et al. 2012, Li, Ma et al. 2012). CXCR4 signaling can induce epithelial-mesenchymal transition in squamous cell carcinoma (Onoue, Uchida et al. 2006). Interestingly, von Hippel-Lindau tumor suppressor (pVHL) can down-regulate CXCR4 and coordinately regulate MMP2/MMP9 expression (Staller, Sulitkova et al. 2003, Struckmann, Mertz et al. 2008). CXCR7 can heterodimerize with CXCR4 and both receptors share the same ligand, CXCL12. CXCR7 was also shown to induce EMT in bladder cancer (Hao, Zheng et al. 2012). Fibronectin (encoded by *FN1*) is a glycoprotein expressed at the cell surface and in the extracellular matrix, and Vimentin (encoded by *VIM*) is a type III intermediate filament and part of the cytoskeleton of mesenchymal cells and is also known as a classical EMT marker (Chaw, Majeed et al. 2012). Both fibronectin and vimentin levels

were reported to increase during the process of EMT (Mani, Guo et al. 2008).

During our project, one study also validated increased expression of some mesenchymal markers in RCC by immunohistology (Harada, Miyake et al. 2012). In addition, EMT in RCC was reported to be regulated by tumor necrosis factor-alpha microRNA-30c and microRNA-200s (Ho, Tang et al. 2012, Huang, Yao et al. 2013, Yoshino, Enokida et al. 2013). Taken together, our results and the recent literature support the hypothesis that EMT plays an important role in the biology of RCC.

4.2 Prognostic significance of EMT genes in primary RCC tumors

The EMT process induces enhanced cell invasion, dissemination of tumor cells and metastasis by a switch from an epithelial to a more sarcomatoid phenotype. Therefore, it is not unexpected that higher levels of EMT-associated gene products have been found to represent markers for poor prognosis in a number of solid tumors (Iwatsuki, Mimori et al. 2010). This has also been noted in RCC patients for selected EMT-associated genes in this study and by other groups (Kallakury, Karikehalli et al. 2001, Cho, Shim et al. 2003, Bandiera, Melloni et al. 2009, Mikami, Katsube et al. 2011, Harada, Miyake et al. 2012). We found significantly reduced tumor-specific survival for higher mRNA expression of *CXCR4*, *VIM, FN1* and *TWIST* (Figure 8). Earlier tumor progression or reduced tumor-specific survival was also reported for elevated expression levels of TWIST, VIM, FN1, MMP2 as well as for SNAI1 and SNAI2 protein levels as determined by immunohistology for patients with clear cell RCC (Yang, Sun et al. 2010, Mikami, Katsube et al. 2011, Harada, Miyake et al. 2012, Steffens, Schrader et al. 2012). Some of these proteins are functionally linked to tumor progression like the transcription factors SNAI1, SNAI2 and TWIST which are key inducers of EMT genes. VIM and the metalloproteinase MMP2 are responsible for adhesion, migration and survival and degradation of the extracellular matrix as well as the basal

membrane, respectively, and therefore instrumental for invasive growth (Orlichenko and Radisky 2008, Yamasaki, Seki et al. 2012, De Craene and Berx 2013).

In summary, EMT represents a process which facilitates the progression of tumors. The results of this study demonstrate that a higher expression of EMT markers indicates worse outcome in RCC patients. CXCR4 and VIM were independent prognostic factors for tumor-specific survival. This result might be useful for clinical outcome evaluation and precise risk stratification of RCC patients, a precondition for an individualized therapeutic strategy.

4.3 Reduced expression of EMT genes and reversal cadherin switch indicates MET in RCC metastasis

E-cadherin is an epithelial adhesin, down-regulated when EMT takes place, while N-cadherin functions as a mesenchymal adhesion molecule, which is supposed to be up-regulated during tumor progression (Araki, Shimura et al. 2011). This is consistent with the loss of polarity and the gain of migratory capacity associated with tumor progression. This E-cadherin/N-cadherin switch was found to be an important signal for EMT and has been proven to be responsible for the progression of prostate cancer (Tomita, van Bokhoven et al. 2000, Gravdal, Halvorsen et al. 2007).

The prognostic power of EMT gene expression to predict tumor-specific survival of RCC patients appears to be lost in metastases samples. This might be explained by the fact that metastasis rarely occurs from metastases (Klein 2009), and EMT gene expression does not necessarily enhance growth of metastases (Tsai, Donaher et al. 2012). Rather reversal of EMT i.e. mesenchymal-epithelial transition (MET) seems to be important for disseminated tumor cells for the establishment of macro-metastases (Tsai, Donaher et al. 2012). Indeed, some EMT associated genes (*ZEB1, CDH2, CXCR7*) seem to be down-regulated in metastases

compared to primary tumors, most notably the CDH2/CDH1 expression ratio which is elevated in primary RCC is significantly smaller in metastases which would be indicative of MET to occur in RCC metastases. Through the dynamic regulation of EMT-related microRNAs or ZEB1/2 (Kurahara, Takao et al. 2012, Yoshino, Enokida et al. 2013), E-cadherin to N-cadherin switch represents the manifestations of EMT, and MET is represented by the N-cadherin to E-cadherin switch accordingly. Two studies of RCC in colorectal cancer (Brabletz, Hlubek et al. 2005, Spaderna, Schmalhofer et al. 2007) showed that MET is detectable in metastasis of colorectal cancer which favors the differentiation of primary tumor cells to finally form metastasis in the colonized area.

In RCC, no study to our knowledge has included samples from metastases for analyzing the expression of EMT genes. This is the first study on this topic and still much is unknown. Further investigations are needed to clarify the role of EMT and MET in RCC metastases, but the results of this study support the hypothesis that MET occurs in RCC metastases.

4.4 G1 and G3 primary tumor share similar expression pattern of the EMT gene set

No significant enrichment of the EMT gene transcripts has been found in G3 compared to G1 primary tumors (Figure 2). Hence, the less differentiated state in G3 tumors does not necessarily correspond to a shift towards an EMT gene expression pattern. However, in clear cell RCC with both carcinomatous and sarcomatous components, the E-cadherin to N-cadherin switching as well as elevated expression of SNAIL and secreted protein acidic and rich in cysteine (SPARC), another typical EMT protein (Table 6), has been described to occur preferentially in the sarcomatoid tumor component (Conant, Peng et al. 2011).

4.5 CXCR4: a link between EMT and cancer stem cell properties in RCC

The metastatic cascade appears to be highly inefficient and only a small proportion of cancer cells are responsible for cell seeding to metastatic sites. Recent studies suggest that this small subpopulation of carcinoma cells exhibit cancer stem cell properties thus linking cancer stem cells to metastasis (Sampieri and Fodde 2012). It has been proposed that carcinoma cells undergo a characteristic change from an epithelial to a mesenchymal cell-like phenotype during cancer progression (Tiwari, Gheldof et al. 2012). This process of epithelial-mesenchymal transition (EMT) involves reduction of cell-cell adhesion and acquisition of invasive properties. Cells undergoing EMT or gaining stem cell properties are sharing similar cell phenotype changes, and both lead to tumor progression and metastases formation.

A link between the EMT phenotype and cancer stem cell properties has been suggested previously (Mani, Guo et al. 2008, Singh and Settleman 2010). We have shown recently that CXCR4 represents a marker for cancer stem cells and is important for their maintenance in RCC cell lines (Gassenmaier, Chen et al. 2013). Besides RCC, CXCR4 is also recognized as stem cell marker in breast and prostate cancer (Dubrovska, Elliott et al. 2012, Dubrovska, Hartung et al. 2012). In addition, CXCR4 signaling can induce EMT as shown for pancreatic cancer cells (Li, Ma et al. 2012). CXCR4 can be down-regulated by the von Hippel-Lindau tumor suppressor pVHL (Staller, Sulitkova et al. 2003, Struckmann, Mertz et al. 2008) and higher expression of CXCR4 predicts poor prognosis in renal cell carcinoma (D'Alterio, Consales et al. 2010). This can be explained by the cancer stem cell properties mediated by high level of CXCR4 (Singh, Singh et al. 2004). Up-regulation of CXCR4 is also accompanied with epithelial-mesenchymal transition and induces cell invasion in pancreatic cancer and oral squamous cell carcinoma (Onoue, Uchida et al. 2006, Taki,

Higashikawa et al. 2008, Li, Ma et al. 2012). These findings suggest that CXCR4 might also be a link between EMT and cancer stem cells in RCC.

In this study, it could be shown that CXCR4 has a significantly increased expression in RCC primary tumors and metastases at both the mRNA and protein level. Furthermore, CXCR4 expression was a significant prognostic marker for tumor-specific survival in univariate analysis as well as an independent prognostic marker in the multivariate Cox regression model. According to the previous finding that CXCR4-positive cells represent cancer stem cells in RCC, it can be concluded that higher CXCR4 expression is directly correlated with the tumor cell capability of cell renewal, migration, invasion and metastasis.

Since cancer stem cells are often more resistant to drugs, CXCR4-targeted molecules could be used for the therapy of RCC. Such therapies could target the CXCR4 signaling pathway in combination with e.g. anti-angiogenic therapies commonly used in patients with advanced disease (Gonzalez Larriba, Espinosa et al. 2012, Domanska, Kruizinga et al. 2013).

4.6 No defined sub-population of CXCR4+/ TPBG+ cells were observed in RCC cell line

TPBG shows increased expression and prognostic significance in malignant pleural mesothelioma (Al-Taei, Salimu et al. 2012), leukemia (Castro, McGinn et al. 2012), cervical cancer (Jones, Roberts et al. 1990), gastric cancer (Naganuma, Kono et al. 2002), colorectal cancer (Starzynska, Marsh et al. 1994) and at high level in renal cell carcinoma (Elkord, Shablak et al. 2009). TPBG was used as a target for immunotherapy in renal cell carcinoma in a series of studies (Shaw, Connolly et al. 2007, Tykodi and Thompson 2008, Tykodi, Satoh et al. 2012). Several therapies were developed to target TPBG, such as vaccination with modified vaccinia Ankara-5T4 (Tykodi and Thompson 2008, Hawkins, Macdermott et al. 2009), anti-5T4 antibody (Sapra,

Damelin et al. 2013) and 5T4-based tumor-targeted super-antigens (Shaw, Connolly et al. 2007). Preclinical effects of these drugs were promising and complete clinical evaluation is still ongoing.

It has been reported that E-cadherin stabilizes the cortical actin cytoskeletal arrangement and this prevents cell surface localization of the 5T4 antigen. Interestingly, presentation of the TPBG antigen at the cell surface is accompanied by the mesenchymal phenotype during ES cell differentiation (Ward, Eastham et al. 2006, Eastham, Spencer et al. 2007, Spencer, Eastham et al. 2007). Upon surface localization, TPBG antigen disrupts cell-cell contacts and induces cellular motility in epithelial cells (Carsberg, Myers et al. 1996).

TPBG is important for keeping CXCR4 on the cell surface and for CXCR4-mediated signaling (Southgate, McGinn et al. 2010, McGinn, Marinov et al. 2012), which is reported to be important for metastasis in lung tumors, breast cancers and renal cell carcinomas (Pan, Mestas et al. 2006, Hamatake, Aoki et al. 2009, D'Alterio, Barbieri et al. 2012, Hawkins and Richmond 2012).

According to the finding that CXCR4 is maintained at the cell surface by TPBG which allows progression-related signaling, we assumed that TPBG and CXCR4 are probably co-expressed in certain “sub-populations” on the cell surface, which directly facilitates CXCR4 signaling. Targeting such “sub-population” cells could be promising to inhibit tumor invasion and metastasis.

However, flow cytometry results in two RCC cell lines RCC53 and SK-RC-17 did not support this assumption. No double-positive staining “sub-population” was found in the selected cell lines. A possible explanation of this finding could be as follows:

It might not be necessary for TPBG to be expressed on the cell surface to maintain the surface expression of CXCR4. It is found that the proportions

of TPBG and CXCR4 are different and are not correlated in different cell lines: in RCC53, 11% of cells are TPBG-positive and only 3.2% of cells are CXCR4-positive; in SK-RC-17, 0.3% of cells are TPBG-positive and around 1.4% of cells are CXCR4-positive. The surface expressions of these two molecules are not correlated with each other. Since there appears to have a functional connection between them, it is assumed that during the maintanace of CXCR4 surface expression, all TPBG molecules are not necessary to be on the outer cell membrane, but might also be in intracellular compartments where it could interact with CXCR4. However, this assumption has to be proven by additional studies about the mode of interaction between the two molecules. In one study on small cell lung cancer cell line H1048, TPBG knockdown using shRNA did not affect the surface expression of CXCR4 (McGinn, Marinov et al. 2012), while the surface expression of TPBG obviously decreased. This result partially supports the finding in this study.

4.7 High expression of ATAD2, TET3, HELLS and TOP2A are independent predictors of poor outcome in RCC patients

Additionally to the focus on EMT- and cancer stem cell-related genes, a novel filtering strategy was used on oligonucleotide microarray data to identify potential new prognostic markers. Genes with increasing expression during tumor progression (expression in normal kidney < in primary tumor < in metastases) could be essential for a malignant phenotype and could therefore have influence on the patients' outcome. Such genes were selected from the array data and analyzed by univariate analysis. The best candidate genes were then validated by RT-PCR. Using this strategy, ATAD2, TET3, HELLS and TOP2A could be identified as independent prognostic markers for tumor-specific survival of RCC patients.

ATAD2, as a tumor-promoting factor cooperating with a series of transcription factors including MYC (Ciro, Prosperini et al. 2009), is up-regulated in many cancers and predicts poor prognosis in osteosarcoma, breast cancer and lung cancer (Fellenberg, Bernd et al. 2007, Caron, Lestrat et al. 2010). TET3, a member of the ten-eleven translocation (TET) gene family, is an epigenetic mediator which plays a role in DNA demethylation. HELLS, encoding a lymphoid-specific helicase, play an essential role in normal development and cell survival through DNA methylation (Myant and Stancheva 2008). HELLS was also identified as a cancer progression marker in head and neck squamous cell carcinoma (Waseem, Ali et al. 2010). TOP2A, which was examined in bladder cancer and breast cancer to be co-amplified with the HER2 oncogene (Bofin, Ytterhus et al. 2003, Simon, Atefy et al. 2003), is also a proliferation-related and prognosis-predicting gene in breast cancer and colorectal cancer (Yang and Jia 2010, Zaczek, Markiewicz et al. 2012).

Up to date, no publication combining any of these four genes with RCC was found. Further studies on these potential novel prognostic markers for RCC are needed to confirm their role in RCC biology.

5. Summary

The clinical course of renal cell carcinoma (RCC) shows a high variability. Prognostic markers are essential to enable an individualized therapeutic strategy. The objective of this study was the identification of novel independent prognostic markers and potential therapeutic targets in RCC. The focus was on genes involved in epithelial-mesenchymal transition (EMT) and cancer stem cell biology.

EMT enhances tumor cell motility and hence plays a critical role in invasion and metastasis in various carcinomas. A set of transcription factors acts as master regulators of EMT. Whether EMT is important for tumor progression in clear cell renal cell carcinoma (RCC) is unknown. Therefore, EMT-related genes were selected from the literature, and their role and prognostic relevance in RCC were analyzed. The known cancer stem cell marker CXCR4 and the associated TPBG gene were also analyzed in this project. Additionally, a novel filter strategy was used to analyze RCC oligonucleotide microarray data for identification of potential prognostic markers: genes with increasing expression during tumor progression (normal kidney < primary tumor < metastases) were selected for outcome analysis because they could be crucial for RCC biology.

Expression of 46 EMT-related genes was analyzed using oligonucleotide microarrays and gene set enrichment analysis (GSEA) in tissue samples from normal kidney and G1 and G3 primary RCC, 14 samples each. Expression of selected EMT genes was validated by real-time polymerase chain reaction (PCR) in normal kidney, primary RCC and metastases in an independent cohort of 112 patients and then combined with follow-up data for survival analysis. Immunohistochemistry, Western blot and flow cytometry were performed to further examine the expression of CXCR4

and co-expression of CXCR4 and TPBG on the surface of RCC cells. GSEA and dChip software were used for microarray data analysis.

The EMT gene set was preferentially expressed in primary tumors compared to normal tissue (false discovery rate FDR=0.01), but no difference between G1 and G3 tumors was found. Quantitative RT-PCR showed down-regulation of critical EMT genes like CDH2 and ZEB1 in metastases which suggests reversal of EMT during metastasis. Kaplan-Meier analysis demonstrated a significant better outcome for patients with low CXCR4, vimentin, fibronectin and TWIST1 mRNA levels. Multivariate analysis revealed that CXCR4 and vimentin up-regulation represent independent prognostic markers for poor cancer-specific survival of RCC patients. The microarray approach using filtering and further RT-PCR validation of progression-associated genes revealed that ATAD2, TET3, HELLS and TOP2A are independent and previously unknown predictors of poor outcome in RCC patients.

Taken together, this study provides strong evidence that EMT occurs in RCC. Modulation of EMT in RCC, therefore, might represent a future therapeutic option. Expression levels of a number of EMT-related genes (like the genes encoding the cancer stem cell marker CXCR4 and vimentin) could be identified as independent prognostic markers. Using a novel filtering approach on array data, additional novel prognostic markers could be identified. These findings contribute to a better risk stratification of RCC patients that can support an individualized and optimized therapeutic strategy.

6. Zusammenfassung

Der klinische Verlauf des Nierenzellkarzinoms (RCC) zeigt eine hohe Variabilität. Prognostische Marker sind unerlässlich, um eine individuelle Therapiestrategie zu ermöglichen. Das Ziel dieser Studie war die Identifizierung neuer unabhängiger prognostischer Marker und potentieller therapeutischer Targets beim RCC. Der Schwerpunkt lag auf Genen, die bei der Epithelial-Mesenchymalen Transition (EMT) und Tumorstammzellenbiologie beteiligt sind.

EMT steigert die Beweglichkeit von Tumorzellen und spielt eine entscheidende Rolle bei der Invasion und Metastasierung bei verschiedenen Karzinomen. Eine Reihe von Transkriptionsfaktoren fungiert als die Hauptregulatoren von EMT. Ob EMT wichtig ist für die Tumorprogression beim klarzelligen Nierenzellkarzinom (RCC), ist unbekannt. Daher wurden EMT-Gene aus der Literatur ausgewählt und ihre Rolle und prognostische Relevanz bei RCC wurden analysiert. Der bekannte Tumorstammzellmarker CXCR4 und das damit assoziierte TPBG-Gen wurden auch in diesem Projekt analysiert. Zusätzlich wurde eine neuartige Filter-Strategie bei RCC-Microarray-Daten verwendet, um mögliche prognostische Marker zu identifizieren: Gene mit zunehmender Expression während der Tumorprogression (normale Niere < Primärtumor < Metastasen) wurden für die Outcome-Analyse ausgewählt, weil sie entscheidend für die RCC-Biologie sein könnten.

Die Expression von 46 EMT-Genen wurde mit Oligonukleotid-Microarrays und *Gene Set Enrichment Analysis* (GSEA) an Gewebeproben von normaler Niere und G1 und G3 Primärtumoren (jeweils 14 Proben) analysiert. Die Expression von ausgewählten EMT-Genen wurde mittels RT-PCR in normaler Niere, primärem RCC und Metastasen an einer unabhängigen Kohorte von 112 Patienten validiert und dann mit Follow-

up-Daten für die Survivalanalyse kombiniert. Immunhistochemie, Western Blot und Durchflusszytometrie wurden durchgeführt, um die Expression von CXCR4 und die Co-Expression von CXCR4 und TPBG auf der Oberfläche von RCC-Zellen weiter zu untersuchen. Die Software GSEA und dChip wurde für die Analyse der Microarray-Daten verwendet.

Das EMT-*gene set* wurde bevorzugt in Primärtumoren exprimiert, verglichen mit dem Normalgewebe (*false discovery rate* FDR = 0,01), es wurde aber kein Unterschied zwischen G1- und G3-Tumoren gefunden. Quantitative RT-PCR zeigte Herunterregulation von kritischen EMT-Genen wie *CDH2* und *ZEB1* in Metastasen, was eine Umkehrung der EMT während der Metastasierung vermuten lässt. Die Kaplan-Meier-Analyse zeigte signifikant bessere Ergebnisse für die Patienten mit niedriger CXCR4, Vimentin, Fibronectin und TWIST1 mRNA Expression. Die multivariate Analyse zeigte, dass eine Hochregulierung von CXCR4 und Vimentin unabhängige prognostischer Marker darstellen für ein schlechtes tumorspezifisches Überleben von RCC-Patienten. Der Microarray-Ansatz mit Filtern und weiterer RT-PCR-Validierung der Progressions-assoziierten Gene ergab, dass ATAD2, TET3, HELLS und TOP2A unabhängige und bisher unbekannte Prädiktoren für schlechtes Outcome bei RCC-Patienten sind.

Insgesamt liefert diese Studie deutliche Hinweise, dass EMT bei RCC vorkommt. Die Modulation von EMT bei RCC könnte daher eine zukünftige therapeutische Option darstellen. Die Expressionsstärke einiger EMT-Gene (z.B. die Gene für den Tumorstammzellmarker CXCR4 und Vimentin) konnten als unabhängige prognostische Marker identifiziert werden. Mit Hilfe eines neuartigen Filter-Ansatzes bei Array-Daten konnten zusätzliche neue prognostische Marker identifiziert werden. Diese Ergebnisse tragen bei zu einer besseren Risikostratifizierung von RCC-Patienten, was eine individualisierte und optimierte Therapiestrategie unterstützen kann.

7. References

Ahmed, N., K. Abubaker, J. Findlay and M. Quinn (2010). "Epithelial mesenchymal transition and cancer stem cell-like phenotypes facilitate chemoresistance in recurrent ovarian cancer." Curr Cancer Drug Targets **10**(3): 268-278.

Aigner, K., B. Dampier, L. Descovich, M. Mikula, A. Sultan, M. Schreiber, W. Mikulits, T. Brabletz, D. Strand, P. Obrist, W. Sommergruber, N. Schweifer, A. Wernitznig, H. Beug, R. Foisner and A. Eger (2007). "The transcription factor ZEB1 (deltaEF1) promotes tumour cell dedifferentiation by repressing master regulators of epithelial polarity." Oncogene **26**(49): 6979-6988.

Aktas, B., M. Tewes, T. Fehm, S. Hauch, R. Kimmig and S. Kasimir-Bauer (2009). "Stem cell and epithelial-mesenchymal transition markers are frequently overexpressed in circulating tumor cells of metastatic breast cancer patients." Breast Cancer Res **11**(4): R46.

Al-Taei, S., J. Salimu, J. F. Lester, S. Linnane, M. Goonewardena, R. Harrop, M. D. Mason and Z. Tabi (2012). "Overexpression and potential targeting of the oncofoetal antigen 5T4 in malignant pleural mesothelioma." Lung Cancer **77**(2): 312-318.

Araki, K., T. Shimura, H. Suzuki, S. Tsutsumi, W. Wada, T. Yajima, T. Kobayahi, N. Kubo and H. Kuwano (2011). "E/N-cadherin switch mediates cancer progression via TGF-beta-induced epithelial-to-mesenchymal transition in extrahepatic cholangiocarcinoma." Br J Cancer **105**(12): 1885-1893.

Asiedu, M. K., J. N. Ingle, M. D. Behrens, D. C. Radisky and K. L. Knutson (2011). "TGFbeta/TNF(alpha)-mediated epithelial-mesenchymal transition generates breast cancer stem cells with a claudin-low phenotype." Cancer Res **71**(13): 4707-4719.

Bandiera, A., G. Melloni, M. Freschi, M. Giovanardi, A. Carretta, A. Borri, P. Ciriaco and P. Zannini (2009). "Prognostic factors and analysis of S100a4 protein in resected pulmonary metastases from renal cell carcinoma." World J Surg **33**(7): 1414-1420.

Bofin, A. M., B. Ytterhus and B. M. Hagmar (2003). "TOP2A and HER-2 gene amplification in fine needle aspirates from breast carcinomas." Cytopathology **14**(6): 314-319.

Boyer, B., G. C. Tucker, A. Delouvee, J. P. Ouhayoun and J. P. Thiery (1988). "Cell adhesion systems: molecular structure and function in embryogenesis and metastasis." Adv Exp Med Biol **233**: 235-244.

Brabletz, T. (2012). "To differentiate or not--routes towards metastasis." Nat Rev Cancer **12**(6): 425-436.

Brabletz, T., F. Hlubek, S. Spaderna, O. Schmalhofer, E. Hiendlmeyer, A. Jung and T. Kirchner (2005). "Invasion and metastasis in colorectal cancer: epithelial-mesenchymal transition, mesenchymal-epithelial transition, stem cells and beta-catenin." Cells Tissues Organs **179**(1-2): 56-65.

Caron, C., C. Lestrat, S. Marsal, E. Escoffier, S. Curtet, V. Virolle, P. Barbry, A. Debernardi, C. Brambilla, E. Brambilla, S. Rousseaux and S. Khochbin (2010). "Functional characterization of ATAD2 as a new cancer/testis factor and a predictor of poor prognosis in breast and lung cancers." Oncogene **29**(37): 5171-5181.

Carsberg, C. J., K. A. Myers and P. L. Stern (1996). "Metastasis-associated 5T4 antigen disrupts cell-cell contacts and induces cellular motility in epithelial cells." Int J Cancer **68**(1): 84-92.

Castro, F. V., O. J. McGinn, S. Krishnan, G. Marinov, J. Li, A. J. Rutkowski, E. Elkord, D. J. Burt, M. Holland, R. Vaghjiani, A. Gallego, V. Saha and P. L. Stern (2012). "5T4 oncofetal antigen is expressed in high risk of relapse childhood pre-B acute lymphoblastic leukemia and is associated with a more invasive and chemotactic phenotype." Leukemia **26**(7): 1487-1498.

Chaw, S. Y., A. A. Majeed, A. J. Dalley, A. Chan, S. Stein and C. S. Farah (2012). "Epithelial to mesenchymal transition (EMT) biomarkers--E-cadherin, beta-catenin, APC and Vimentin--in oral squamous cell carcinogenesis and transformation." Oral Oncol **48**(10): 997-1006.

Cho, N. H., H. S. Shim, S. Y. Rha, S. H. Kang, S. H. Hong, Y. D. Choi, S. J. Hong and S. H. Cho (2003). "Increased expression of matrix metalloproteinase 9 correlates with poor prognostic variables in renal cell carcinoma." Eur Urol **44**(5): 560-566.

Ciro, M., E. Prosperini, M. Quarto, U. Grazini, J. Walfridsson, F. McBlane, P. Nucifero, G. Pacchiana, M. Capra, J. Christensen and K. Helin (2009). "ATAD2 is a novel cofactor for MYC, overexpressed and amplified in aggressive tumors." Cancer Res **69**(21): 8491-8498.

Conant, J. L., Z. Peng, M. F. Evans, S. Naud and K. Cooper (2011). "Sarcomatoid renal cell carcinoma is an example of epithelial--mesenchymal transition." J Clin Pathol **64**(12): 1088-1092.

D'Alterio, C., A. Barbieri, L. Portella, G. Palma, M. Polimeno, A. Riccio, C. Ierano, R. Franco, G. Scognamiglio, J. Bryce, A. Luciano, D. Rea, C. Arra and S. Scala (2012). "Inhibition of stromal CXCR4 impairs development of lung metastases." Cancer Immunol Immunother.

D'Alterio, C., C. Consales, M. Polimeno, R. Franco, L. Cindolo, L. Portella, M. Cioffi, R. Calemma, L. Marra, L. Claudio, S. Perdona, S. Pignata, G. Facchini, G. Carteni, N. Longo, L. Pucci, A. Ottaiano, S. Costantini, G. Castello and S. Scala (2010). "Concomitant CXCR4 and CXCR7 expression predicts poor prognosis in renal cancer." Curr Cancer Drug Targets **10**(7): 772-781.

De Craene, B. and G. Berx (2013). "Regulatory networks defining EMT during cancer initiation and progression." Nat Rev Cancer **13**(2): 97-110.

Djafarzadeh, R., E. Noessner, H. Engelmann, D. J. Schendel, M. Notohamiprodjo, I. von Luettichau and P. J. Nelson (2006). "GPI-anchored TIMP-1 treatment renders renal cell carcinoma sensitive to FAS-meditated killing." Oncogene **25**(10): 1496-1508.

Domanska, U. M., R. C. Kruizinga, W. B. Nagengast, H. Timmer-Bosscha, G. Huls, E. G. de Vries and A. M. Walenkamp (2013). "A review on CXCR4/CXCL12 axis in oncology: no place to hide." Eur J Cancer **49**(1): 219-230.

Dubrovska, A., J. Elliott, R. J. Salamone, G. D. Telegeev, A. E. Stakhovsky, I. B. Schepotin, F. Yan, Y. Wang, L. C. Bouchez, S. A. Kularatne, J. Watson, C. Trussell, V. A. Reddy, C. Y. Cho and P. G. Schultz (2012). "CXCR4 expression in prostate cancer progenitor cells." PLoS One **7**(2): e31226.

Dubrovska, A., A. Hartung, L. C. Bouchez, J. R. Walker, V. A. Reddy, C. Y. Cho and P. G. Schultz (2012). "CXCR4 activation maintains a stem cell population in tamoxifen-resistant breast cancer cells through AhR signalling." Br J Cancer **107**(1): 43-52.

Eastham, A. M., H. Spencer, F. Soncin, S. Ritson, C. L. Merry, P. L. Stern and C. M. Ward (2007). "Epithelial-mesenchymal transition events during human embryonic stem cell differentiation." Cancer Res **67**(23): 11254-11262.

Ebert, T., N. H. Bander, C. L. Finstad, R. D. Ramsawak and L. J. Old (1990). "Establishment and characterization of human renal cancer and normal kidney cell lines." Cancer Res **50**(17): 5531-5536.

Elkord, E., A. Shablak, P. L. Stern and R. E. Hawkins (2009). "5T4 as a target for immunotherapy in renal cell carcinoma." Expert Rev Anticancer Ther **9**(12): 1705-1709.

Fellenberg, J., L. Bernd, G. Delling, D. Witte and A. Zahlten-Hinguranage (2007). "Prognostic significance of drug-regulated genes in high-grade osteosarcoma." Mod Pathol **20**(10): 1085-1094.

Gassenmaier, M., D. Chen, A. Buchner, L. Henkel, M. Schiemann, B. Mack, D. J. Schendel, W. Zimmermann and H. Pohla (2013). "CXC chemokine receptor 4 is essential for maintenance of renal cell carcinoma-initiating cells and predicts metastasis." Stem Cells.

Geiger, T. R. and D. S. Peeper (2009). "Metastasis mechanisms." Biochim Biophys Acta **1796**(2): 293-308.

Gonzalez Larriba, J. L., E. Espinosa, I. Garcia Carbonero, J. Garcia-Donas, M. Lopez, A. Meana, J. Puente and J. Bellmunt (2012). "Sequential therapy in metastatic renal cell carcinoma: pre-clinical and clinical rationale for selecting a second- or subsequent-line therapy with a different mechanism of action." Cancer Metastasis Rev **31 Suppl 1**: S11-17.

Gravdal, K., O. J. Halvorsen, S. A. Haukaas and L. A. Akslen (2007). "A switch from E-cadherin to N-cadherin expression indicates epithelial to mesenchymal transition and is of strong and independent importance for the progress of prostate cancer." Clin Cancer Res **13**(23): 7003-7011.

Hamatake, M., T. Aoki, Y. Futahashi, E. Urano, N. Yamamoto and J. Komano (2009). "Ligand-independent higher-order multimerization of CXCR4, a G-protein-coupled chemokine receptor involved in targeted metastasis." Cancer Sci **100**(1): 95-102.

Hao, M., J. Zheng, K. Hou, J. Wang, X. Chen, X. Lu, J. Bo, C. Xu, K. Shen and J. Wang (2012). "Role of chemokine receptor CXCR7 in bladder cancer progression." Biochem Pharmacol **84**(2): 204-214.

Harada, K., H. Miyake, Y. Kusuda and M. Fujisawa (2012). "Expression of epithelial-mesenchymal transition markers in renal cell carcinoma: impact on prognostic outcomes in patients undergoing radical nephrectomy." BJU Int **110**(11 Pt C): E1131-1137.

Hawkins, O. E. and A. Richmond (2012). "The dynamic yin-yang interaction of CXCR4 and CXCR7 in breast cancer metastasis." Breast Cancer Res **14**(1): 103.

Hawkins, R. E., C. Macdermott, A. Shablak, C. Hamer, F. Thistlethwaite, N. L. Drury, P. Chikoti, W. Shingler, S. Naylor and R. Harrop (2009). "Vaccination of patients with metastatic renal cancer with modified vaccinia Ankara encoding the tumor antigen 5T4 (TroVax) given alongside interferon-alpha." J Immunother **32**(4): 424-429.

Haynes, J., J. Srivastava, N. Madson, T. Wittmann and D. L. Barber (2011). "Dynamic actin remodeling during epithelial-mesenchymal transition depends on increased moesin expression." Mol Biol Cell **22**(24): 4750-4764.

Heldin, C. H., M. Vanlandewijck and A. Moustakas (2012). "Regulation of EMT by TGFbeta in cancer." FEBS Lett **586**(14): 1959-1970.

Ho, M. Y., S. J. Tang, M. J. Chuang, T. L. Cha, J. Y. Li, G. H. Sun and K. H. Sun (2012). "TNF-alpha induces epithelial-mesenchymal transition of renal cell carcinoma cells via a GSK3beta-dependent mechanism." Mol Cancer Res **10**(8): 1109-1119.

Huang, J., X. Yao, J. Zhang, B. Dong, Q. Chen, W. Xue, D. Liu and Y. Huang (2013). "Hypoxia-induced downregulation of miR-30c promotes epithelial-mesenchymal transition in human renal cell carcinoma." Cancer Sci.

Iwatsuki, M., K. Mimori, T. Yokobori, H. Ishi, T. Beppu, S. Nakamori, H. Baba and M. Mori (2010). "Epithelial-mesenchymal transition in cancer development and its clinical significance." Cancer Sci **101**(2): 293-299.

Jones, H., G. Roberts, N. Hole, I. W. McDicken and P. Stern (1990). "Investigation of expression of 5T4 antigen in cervical cancer." Br J Cancer **61**(1): 96-100.

Kallakury, B. V., S. Karikehalli, A. Haholu, C. E. Sheehan, N. Azumi and J. S. Ross (2001). "Increased expression of matrix metalloproteinases 2 and 9 and tissue inhibitors of metalloproteinases 1 and 2 correlate with poor prognostic variables in renal cell carcinoma." Clin Cancer Res **7**(10): 3113-3119.

Kalluri, R. and E. G. Neilson (2003). "Epithelial-mesenchymal transition and its implications for fibrosis." J Clin Invest **112**(12): 1776-1784.

Kalluri, R. and R. A. Weinberg (2009). "The basics of epithelial-mesenchymal transition." J Clin Invest **119**(6): 1420-1428.

Klein, C. A. (2009). "Parallel progression of primary tumours and metastases." Nat Rev Cancer **9**(4): 302-312.

Kurahara, H., S. Takao, K. Maemura, Y. Mataki, T. Kuwahata, K. Maeda, Q. Ding, M. Sakoda, S. Iino, S. Ishigami, S. Ueno, H. Shinchi and S. Natsugoe (2012). "Epithelial-mesenchymal transition and mesenchymal-epithelial transition via regulation of ZEB-1 and ZEB-2 expression in pancreatic cancer." J Surg Oncol **105**(7): 655-661.

Li, C. and W. H. Wong (2001). "Model-based analysis of oligonucleotide arrays: expression index computation and outlier detection." Proc Natl Acad Sci U S A **98**(1): 31-36.

Li, X., Q. Ma, Q. Xu, H. Liu, J. Lei, W. Duan, K. Bhat, F. Wang, E. Wu and Z. Wang (2012). "SDF-1/CXCR4 signaling induces pancreatic cancer cell invasion and epithelial-mesenchymal transition in vitro through non-canonical activation of Hedgehog pathway." Cancer Lett **322**(2): 169-176.

Liu, Y., S. El-Naggar, D. S. Darling, Y. Higashi and D. C. Dean (2008). "Zeb1 links epithelial-mesenchymal transition and cellular senescence." Development **135**(3): 579-588.

Ljungberg, B., S. C. Campbell, H. Y. Choi, D. Jacqmin, J. E. Lee, S. Weikert and L. A. Kiemeney (2011). "The epidemiology of renal cell carcinoma." Eur Urol **60**(4): 615-621.

Mani, S. A., W. Guo, M. J. Liao, E. N. Eaton, A. Ayyanan, A. Y. Zhou, M. Brooks, F. Reinhard, C. C. Zhang, M. Shipitsin, L. L. Campbell, K. Polyak, C. Brisken, J. Yang and R. A. Weinberg (2008). "The epithelial-mesenchymal transition generates cells with properties of stem cells." Cell **133**(4): 704-715.

Maruschke, M., O. W. Hakenberg, D. Koczan, W. Zimmermann, C. G. Stief and A. Buchner (2013). "Expression profiling of metastatic renal cell carcinoma using gene set enrichment analysis." Int J Urol.

McGinn, O. J., G. Marinov, S. Sawan and P. L. Stern (2012). "CXCL12 receptor preference, signal transduction, biological response and the expression of 5T4 oncofoetal glycoprotein." J Cell Sci **125**(Pt 22): 5467-5478.

Mikami, S., K. Katsube, M. Oya, M. Ishida, T. Kosaka, R. Mizuno, M. Mukai and Y. Okada (2011). "Expression of Snail and Slug in renal cell carcinoma: E-

cadherin repressor Snail is associated with cancer invasion and prognosis." Lab Invest **91**(10): 1443-1458.

Myant, K. and I. Stancheva (2008). "LSH cooperates with DNA methyltransferases to repress transcription." Mol Cell Biol **28**(1): 215-226.

Naganuma, H., K. Kono, Y. Mori, S. Takayoshi, P. L. Stern, K. Tasaka and Y. Matsumoto (2002). "Oncofetal antigen 5T4 expression as a prognostic factor in patients with gastric cancer." Anticancer Res **22**(2B): 1033-1038.

Okada, H., T. M. Danoff, R. Kalluri and E. G. Neilson (1997). "Early role of Fsp1 in epithelial-mesenchymal transformation." Am J Physiol **273**(4 Pt 2): F563-574.

Onoue, T., D. Uchida, N. M. Begum, Y. Tomizuka, H. Yoshida and M. Sato (2006). "Epithelial-mesenchymal transition induced by the stromal cell-derived factor-1/CXCR4 system in oral squamous cell carcinoma cells." Int J Oncol **29**(5): 1133-1138.

Orlichenko, L. S. and D. C. Radisky (2008). "Matrix metalloproteinases stimulate epithelial-mesenchymal transition during tumor development." Clin Exp Metastasis **25**(6): 593-600.

Pan, J., J. Mestas, M. D. Burdick, R. J. Phillips, G. V. Thomas, K. Reckamp, J. A. Belperio and R. M. Strieter (2006). "Stromal derived factor-1 (SDF-1/CXCL12) and CXCR4 in renal cell carcinoma metastasis." Mol Cancer **5**: 56.

Polyak, K. and R. A. Weinberg (2009). "Transitions between epithelial and mesenchymal states: acquisition of malignant and stem cell traits." Nat Rev Cancer **9**(4): 265-273.

Rhim, A. D., E. T. Mirek, N. M. Aiello, A. Maitra, J. M. Bailey, F. McAllister, M. Reichert, G. L. Beatty, A. K. Rustgi, R. H. Vonderheide, S. D. Leach and B. Z. Stanger (2012). "EMT and dissemination precede pancreatic tumor formation." Cell **148**(1-2): 349-361.

Rudland, P. S., A. Platt-Higgins, C. Renshaw, C. R. West, J. H. Winstanley, L. Robertson and R. Barraclough (2000). "Prognostic significance of the metastasis-inducing protein S100A4 (p9Ka) in human breast cancer." Cancer Res **60**(6): 1595-1603.

Sampieri, K. and R. Fodde (2012). "Cancer stem cells and metastasis." Semin Cancer Biol **22**(3): 187-193.

Sapra, P., M. Damelin, J. Dijoseph, K. Marquette, K. G. Geles, J. Golas, M. Dougher, B. Narayanan, A. Giannakou, K. Khandke, R. Dushin, E. Ernstoff, J. Lucas, M. Leal, G. Hu, C. J. O'Donnell, L. Tchistiakova, R. T. Abraham and H. P. Gerber (2013). "Long-term tumor regression induced by an antibody-drug conjugate that targets 5T4, an oncofetal antigen expressed on tumor-initiating cells." Mol Cancer Ther **12**(1): 38-47.

Shaw, D. M., N. B. Connolly, P. M. Patel, S. Kilany, G. Hedlund, O. Nordle, G. Forsberg, J. Zweit, P. L. Stern and R. E. Hawkins (2007). "A phase II study of a 5T4 oncofoetal antigen tumour-targeted superantigen (ABR-214936) therapy in patients with advanced renal cell carcinoma." Br J Cancer **96**(4): 567-574.

Simon, R., R. Atefy, U. Wagner, T. Forster, A. Fijan, J. Bruderer, K. Wilber, M. J. Mihatsch, T. Gasser and G. Sauter (2003). "HER-2 and TOP2A coamplification in urinary bladder cancer." Int J Cancer **107**(5): 764-772.

Singh, A. and J. Settleman (2010). "EMT, cancer stem cells and drug resistance: an emerging axis of evil in the war on cancer." Oncogene **29**(34): 4741-4751.

Singh, S., U. P. Singh, W. E. Grizzle and J. W. Lillard, Jr. (2004). "CXCL12-CXCR4 interactions modulate prostate cancer cell migration, metalloproteinase expression and invasion." Lab Invest **84**(12): 1666-1676.
Sobin L, G. M., Wittekind C (2009). AJCC staging manual, 7th edn, Springer.

Southgate, T. D., O. J. McGinn, F. V. Castro, A. J. Rutkowski, M. Al-Muftah, G. Marinov, G. J. Smethurst, D. Shaw, C. M. Ward and C. J. Miller (2010). "CXCR4 mediated chemotaxis is regulated by 5T4 oncofetal glycoprotein in mouse embryonic cells." PloS one **5**(4): e9982.

Spaderna, S., O. Schmalhofer, F. Hlubek, A. Jung, T. Kirchner and T. Brabletz (2007). "Epithelial-mesenchymal and mesenchymal-epithelial transitions during cancer progression." Verh Dtsch Ges Pathol **91**: 21-28.

Spencer, H. L., A. M. Eastham, C. L. Merry, T. D. Southgate, F. Perez-Campo, F. Soncin, S. Ritson, R. Kemler, P. L. Stern and C. M. Ward (2007). "E-cadherin inhibits cell surface localization of the pro-migratory 5T4 oncofetal antigen in mouse embryonic stem cells." Mol Biol Cell **18**(8): 2838-2851.

Staller, P., J. Sulitkova, J. Lisztwan, H. Moch, E. J. Oakeley and W. Krek (2003). "Chemokine receptor CXCR4 downregulated by von Hippel-Lindau tumour suppressor pVHL." Nature **425**(6955): 307-311.

Starzynska, T., P. J. Marsh, P. F. Schofield, S. A. Roberts, K. A. Myers and P. L. Stern (1994). "Prognostic significance of 5T4 oncofetal antigen expression in colorectal carcinoma." Br J Cancer **69**(5): 899-902.

Steffens, S., A. J. Schrader, G. Vetter, H. Eggers, H. Blasig, J. Becker, M. A. Kuczyk and J. Serth (2012). "Fibronectin 1 protein expression in clear cell renal cell carcinoma." Oncol Lett **3**(4): 787-790.

Struckmann, K., K. Mertz, S. Steu, M. Storz, P. Staller, W. Krek, P. Schraml and H. Moch (2008). "pVHL co-ordinately regulates CXCR4/CXCL12 and MMP2/MMP9 expression in human clear-cell renal cell carcinoma." J Pathol **214**(4): 464-471.

Subramanian, A., P. Tamayo, V. K. Mootha, S. Mukherjee, B. L. Ebert, M. A. Gillette, A. Paulovich, S. L. Pomeroy, T. R. Golub, E. S. Lander and J. P. Mesirov (2005). "Gene set enrichment analysis: a knowledge-based approach for interpreting genome-wide expression profiles." Proc Natl Acad Sci U S A **102**(43): 15545-15550.

Taki, M., K. Higashikawa, S. Yoneda, S. Ono, H. Shigeishi, M. Nagayama and N. Kamata (2008). "Up-regulation of stromal cell-derived factor-1alpha and its receptor CXCR4 expression accompanied with epithelial-mesenchymal transition in human oral squamous cell carcinoma." Oncol Rep **19**(4): 993-998.

Teixido, C., R. Mares, M. Aracil, S. Ramon y Cajal and J. Hernandez-Losa (2013). "Epithelial-mesenchymal transition markers and HER3 expression are predictors of elisidepsin treatment response in breast and pancreatic cancer cell lines." PLoS One **8**(1): e53645.

Teng, Y., M. Zeisberg and R. Kalluri (2007). "Transcriptional regulation of epithelial-mesenchymal transition." J Clin Invest **117**(2): 304-306.

Therneau, T. M., Grambsch, P. M., Fleming, T. R., (1990). "Martingale-based residuals for survival models." Biometrika **77**: 14.

Thiery, J. P., H. Acloque, R. Y. Huang and M. A. Nieto (2009). "Epithelial-mesenchymal transitions in development and disease." Cell **139**(5): 871-890.

Thiery, J. P., B. Boyer, G. Tucker, J. Gavrilovic and A. M. Valles (1988). "Adhesion mechanisms in embryogenesis and in cancer invasion and metastasis." Ciba Found Symp **141**: 48-74.

Thomson, S., F. Petti, I. Sujka-Kwok, P. Mercado, J. Bean, M. Monaghan, S. L. Seymour, G. M. Argast, D. M. Epstein and J. D. Haley (2011). "A systems view of epithelial-mesenchymal transition signaling states." Clin Exp Metastasis **28**(2): 137-155.

Tiwari, N., A. Gheldof, M. Tatari and G. Christofori (2012). "EMT as the ultimate survival mechanism of cancer cells." Semin Cancer Biol **22**(3): 194-207.

Tomita, K., A. van Bokhoven, G. J. van Leenders, E. T. Ruijter, C. F. Jansen, M. J. Bussemakers and J. A. Schalken (2000). "Cadherin switching in human prostate cancer progression." Cancer Res **60**(13): 3650-3654.

Tsai, J. H., J. L. Donaher, D. A. Murphy, S. Chau and J. Yang (2012). "Spatiotemporal regulation of epithelial-mesenchymal transition is essential for squamous cell carcinoma metastasis." Cancer Cell **22**(6): 725-736.

Tykodi, S. S., S. Satoh, J. D. Deming, J. Chou, R. Harrop and E. H. Warren (2012). "CD8+ T-cell clones specific for the 5T4 antigen target renal cell carcinoma tumor-initiating cells in a murine xenograft model." J Immunother **35**(7): 523-533.

Tykodi, S. S. and J. A. Thompson (2008). "Development of modified vaccinia Ankara-5T4 as specific immunotherapy for advanced human cancer." Expert Opin Biol Ther **8**(12): 1947-1953.

Wang, H., R. Fang, X. F. Wang, F. Zhang, D. Y. Chen, B. Zhou, H. S. Wang, S. H. Cai and J. Du (2013). "Stabilization of Snail through AKT/GSK-3beta signaling pathway is required for TNF-alpha-induced epithelial-mesenchymal transition in prostate cancer PC3 cells." Eur J Pharmacol **714**(1-3): 48-55.

Ward, C. M., A. M. Eastham and P. L. Stern (2006). "Cell surface 5T4 antigen is transiently upregulated during early human embryonic stem cell differentiation: effect of 5T4 phenotype on neural lineage formation." Exp Cell Res **312**(10): 1713-1726.

Waseem, A., M. Ali, E. W. Odell, F. Fortune and M. T. Teh (2010). "Downstream targets of FOXM1: CEP55 and HELLS are cancer progression markers of head and neck squamous cell carcinoma." Oral Oncol **46**(7): 536-542.

Xia, H., L. L. Ooi and K. M. Hui (2013). "MicroRNA-216a/217-induced epithelial-mesenchymal transition targets PTEN and SMAD7 to promote drug resistance and recurrence of liver cancer." Hepatology **58**(2): 629-641.

Yamasaki, T., N. Seki, Y. Yamada, H. Yoshino, H. Hidaka, T. Chiyomaru, N. Nohata, T. Kinoshita, M. Nakagawa and H. Enokida (2012). "Tumor suppressive microRNA138 contributes to cell migration and invasion through its targeting of vimentin in renal cell carcinoma." Int J Oncol **41**(3): 805-817.

Yan, S., Y. Wang, Q. Yang, X. Li, X. Kong, N. Zhang, C. Yuan, N. Yang and B. Kong (2013). "Low-dose radiation-induced epithelial-mesenchymal transition through NF-kappaB in cervical cancer cells." Int J Oncol **42**(5): 1801-1806.

Yang, F. D. and Z. L. Jia (2010). "[Expression of topoisomerase II alpha in human colorectal carcinoma and its significance]." Nan Fang Yi Ke Da Xue Xue Bao **30**(8): 1959-1961, 1964.

Yang, M. H., S. Y. Chang, S. H. Chiou, C. J. Liu, C. W. Chi, P. M. Chen, S. C. Teng and K. J. Wu (2007). "Overexpression of NBS1 induces epithelial-mesenchymal transition and co-expression of NBS1 and Snail predicts metastasis of head and neck cancer." Oncogene **26**(10): 1459-1467.

Yang, S. D., R. C. Sun, H. J. Mu, Z. Q. Xu and Z. Y. Zhou (2010). "The expression and clinical significance of TGF-beta1 and MMP2 in human renal clear cell carcinoma." Int J Surg Pathol **18**(2): 85-93.

Yang, X., S. Liu and Q. Yan (2013). "Role of fucosyltransferase IV in epithelial-mesenchymal transition in breast cancer cells." Cell Death Dis **4**: e735.

Ye, J., G. Coulouris, I. Zaretskaya, I. Cutcutache, S. Rozen and T. L. Madden (2012). "Primer-BLAST: a tool to design target-specific primers for polymerase chain reaction." BMC Bioinformatics **13**: 134.

Yoshino, H., H. Enokida, T. Itesako, S. Tatarano, T. Kinoshita, M. Fuse, S. Kojima, M. Nakagawa and N. Seki (2013). "Epithelial-mesenchymal transition-related microRNA-200s regulate molecular targets and pathways in renal cell carcinoma." J Hum Genet **58**(8): 508-516.

Zaczek, A. J., A. Markiewicz, B. Seroczynska, J. Skokowski, J. Jaskiewicz, T. Pienkowski, W. P. Olszewski, J. Szade, P. Rhone, M. Welnicka-Jaskiewicz and J. Jassem (2012). "Prognostic significance of TOP2A gene dosage in HER-2-negative breast cancer." Oncologist **17**(10): 1246-1255.

Zeisberg, M. and E. G. Neilson (2009). "Biomarkers for epithelial-mesenchymal transitions." J Clin Invest **119**(6): 1429-1437.

Zhang, L., Z. Liu, W. Ma and B. Wang (2013). "The landscape of histone acetylation involved in epithelial-mesenchymal transition in lung cancer." J Cancer Res Ther **9 Suppl**: S86-91.

Zhao, L., W. Li, W. Zang, Z. Liu, X. Xu, H. Yu, Q. Yang and J. Jia (2013). "JMJD2B promotes epithelial-mesenchymal transition by cooperating with beta-catenin and enhances gastric cancer metastasis." Clin Cancer Res.

Zhu, Q. C., R. Y. Gao, W. Wu and H. L. Qin (2013). "Epithelial-mesenchymal Transition and Its Role in the Pathogenesis of Colorectal Cancer." Asian Pac J Cancer Prev **14**(5): 2689-2698.

Zhu, Z., Z. Zhu, Z. Pang, Y. Xing, F. Wan, D. Lan and H. Wang (2013). "Short hairpin RNA targeting FOXQ1 inhibits invasion and metastasis via the reversal of epithelial-mesenchymal transition in bladder cancer." Int J Oncol **42**(4): 1271-1278.

8. Abbreviations

7-AAD	7-aminoactinomycin D
ß-ME	beta-mercaptoethanol
CMV	human cytomegalus virus
CSC	cancer stem cell
D	days
DMEM	Dulbecco's modified Eagle's media
DNA	deoxyribonucleic acid
dNTP	Deoxynucleotide_triphosphate
E. coli	*Escherichia coli*
EMT	epithelial-mesenchymal transition
FACS	fluorescence-activated cell sorting
FBS	fetal bovine serum
FGF	fibroblast growth factor
FITC	fluorescein isothiocyanate
GAPDH	glyceraldehyde-3-phosphate-dehydrogenase
H	hour
HRP	horseradish-peroxidase
IgG	immunoglobin G
IHC	immunohistochemistry
Kb	kilobases
kD	kilo Dalton
LB	lysogeny broth
M	mole
MET	mesenchymal-epithelial transition
Mg	milligram
Min	minute
Ml	milliliter
mM	millimolar
mRCC	metastatic renal cell carcinoma
mRNA	messenger ribonucleic acid
µg	microgram

µl	microliter
nm	nanometer
PBS	phosphate-buffered saline
PCR	polymerase chain reaction
qPCR	quantitative polymerase chain reaction
RCC	renal cell carcinoma
RNA	ribonucleic acid
RPMI	Roswell Park Memorial Institute
RT-PCR	real-time reverse transcription PCR
SDS-PAGE	sodium dodecyl sulfate polyacrylamide gel electrophoresis
TBS/T	Tris-buffered saline supplemented with Tween-20
TPBG	trophoblast glycoprotein
Tris	2-amino-2-hydroxymethyl-propane-1,3-diol

9. Acknowledgement

Firstly, I would like to thank Prof. Dr. Christian Stief, my supervisor, for giving me this opportunity to work in the Department of Urology, Klinikum Großhadern as a candidate of doctoral student and finish my thesis under supervision of PD Dr. Buchner, he helped me a lot to support my academic experience as well as a precious chance to experience an amazing life in Munich. Very special thanks go to my co-supervisor Priv. Doz. Dr. med. Buchner for his consistent and always reliable support both in daily life problems and work puzzle. I cannot make it without your supervision and it is such a marvelous life experience I have went through in the lab. My sincere thanks also go to Prof. Dr. rer. nat. Wolfgang Zimmermann for his precise and direct instructions during my project; he is always there for all the students and has such a magic scientific mind to help me to find the tail out of a tangled mess.

My thanks also go to Dr. Rainer Riesenberg, who is always calm and positive and taught me a lot in the technique skills. Also, I would like to thank PD Dr. rer. nat. Heike Pohla and Birgit Stadlbauer for their kindness and help during my work. What is more, they are so sweet and always prepared so many interesting gifts together with joy for everyone in the birthday. I also have to thank all the other doctoral students who are also enjoying and suffering their projects as I do: Max is such an intelligent researcher who does a great job of his project, I learned so much skills and tips of experiments from him and he is always willing to help; Johannes is a sporty and outdoor man who is always full of energy, he is always in the lab as a comrade in arms and encourages me a lot; the ladies Mira, Gabriele, Quynh-Trang, Leonie and Mingqian are so nice and always in the lab when I was seeking for help, they helped me a lot when I encountered experiment problems.

For my project, I sincerely thank Dr. Matthias Maruschke from the University of Rostock who provided his precious microarray data to me to make my project complete and successfully published.

My last thanks go to my big family: my mother dedicates her life for my brother, my sister and me, too many words in the world cannot explain my love for her; my father did hard work to support the family; my parents-in-law gave so many supports and most importantly my dear wife to me; my brother and his wife are always backing up for me and he protected tiny me in my pupil old times; my sister and my two naughty nephews I love them very much; for my darling wife and my treasure "Morning", I owe you my rest life.

My work in the Department of Urology, LMU was supported by scholarship from China Scholarship Council (CSC).

10. Curriculum vitae

NAME Dong Chen

BIRTH Born 18th of October, 1987 in Pingtan, China

CONTACT +49 176 9324 0426

chendongonlyone@gmail.com;

dong.chen@med.uni-muenchen.de

EDUCATION

2011-2014	Department of Urology, Klinikum Großhadern, Ludwig-Maximilians-Universität München, Germany Dr. med. candidate (Major: Urology) Supervisor: Prof. Dr. med. Christian G. Stief Co-supervisor: PD Dr. med. Alexander Buchner
2004-2011	Department of Urology, Zhongnan Hospital of Wuhan University Bachelor & Master in Medicine (Master Major: Urology) Supervisor: Prof. M. D. Xinghuang Wang
2006-2009	Psychology college, Huazhong Normal University Second Bachelor Degree of Psychology

RESEARCH EXPERIENCE

Working as medical student and preparing thesis in laboratories of Medical research center of Zhongnan Hospital (2009-2011) and Department of Urology of Klinikum Großhadern, Ludwig-Maximilians-Universität München (2011-2014).

PUBLICATIONS

Expression and prognostic significance of a comprehensive epithelial-mesenchymal transition gene set in renal cell carcinoma.
Chen D, Gassenmaier M, Maruschke M, Riesenberg R, Pohla H, Stief CG, Zimmermann W, Buchner A.
J Urol. 2014; 191(2): 479-86

CXC chemokine receptor 4 is essential for maintenance of renal cell carcinoma-initiating cells and predicts metastasis.
Gassenmaier M, Chen D, Buchner A, Henkel L, Schiemann M, Mack B, Schendel DJ, Zimmermann W, Pohla H.
Stem Cells. 2013; 31(8):1467-76

Capsaicin induces cycle arrest by inhibiting cyclin-dependent-kinase in bladder carcinoma cells.
Chen D, Yang Z, Wang Y, Zhu G, Wang X.
Int J Urol. 2012 Jul; 19(7):662-8

Effects of TRPM8 on the proliferation and angiogenesis of prostate cancer PC-3 cells in vivo.
Zhu G, Wang X, Yang Z, Cao H, Meng Z, Wang Y, Chen D.
Oncol Lett. 2011 Nov; 2(6):1213-1217

Short hairpin ribonucleic acid constructs targeting insulin-like growth factor binding protein-3 ameliorates diabetes mellitus-related erectile dysfunction in rats.
Yang Z, Zhou Z, Wang X, Peng M, Zhou H, Meng Z, Chen D, Wang Y.
Urology. 2013 Feb; 81(2):464.e11-6

Menthol inhibits the proliferation and motility of prostate cancer DU145 cells.
Wang Y, Wang X, Yang Z, Zhu G, Chen D, Meng Z.
Pathol Oncol Res. 2012 Oct; 18(4):903-10

Effect of surgical castration on expression of TRPM8 in urogenital tract of male rats.
Yang Z, Wang X, Zhu G, Zhou Z, Wang Y, Chen D, Meng Z.
Mol Biol Rep. 2012 Apr; 39(4):4797-802

Increased expression of insulin-like growth factor-binding protein-3 is implicated in erectile dysfunction in two-kidney one-clip hypertensive rats after propranolol treatment.
Zhou ZY, Yang ZH, Wang XH, Cao H, Chen D, Wang YZ, Zhou HH, Peng M, Liu QL, Wan SP.
Asian J Androl. 2011 Nov; 13(6):851-5

11. Eidesstattliche Versicherung und Erklärung

Eidesstattliche Versicherung

Chen, Dong

Name, Vorname

Ich erkläre hiermit an Eides statt,

dass ich die vorliegende Dissertation mit dem Thema

Identification of new prognostic markers in renal cell carcinoma.

selbständig verfasst, mich außer der angegebenen keiner weiteren Hilfsmittel bedient und alle Erkenntnisse, die aus dem Schrifttum ganz oder annähernd übernommen sind, als solche kenntlich gemacht und nach ihrer Herkunft unter Bezeichnung der Fundstelle einzeln nachgewiesen habe.

Ich erkläre des Weiteren, dass die hier vorgelegte Dissertation nicht in gleicher oder in ähnlicher Form bei einer anderen Stelle zur Erlangung eines akademischen Grades eingereicht wurde.

31.03.2014

Ort, Datum

Dong Chen

Unterschrift Doktorandin/Doktorand